CORRELATED MULTI - MYOELECTRIC SIGNAL FORCE SENSOR TO LOAD BEARING

by

BHASKAR PALIT

CORRELATED MULTI - MYOELECTRIC SIGNAL AS FORCE SENSOR TO LOAD BEARING

A Thesis Submitted
in Partial Fulfilment of the Requirements
for the Degree of
MASTER OF TECHNOLOGY

by
BHASKAR PALIT

to the
INDUSTRIAL AND MANAGEMENT ENGINEERING PROGRAMME
INDIAN INSTITUTE OF TECHNOLOGY, KANPUR
AUGUST, 1990

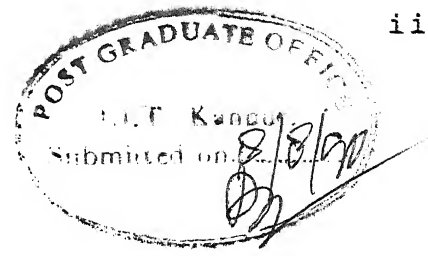

CERTIFICATE

It is certified that this work "CORRELATED MULTI-MYOELECTRIC SIGNAL AS FORCE SENSOR TO LOAD BEARING" by BHASKAR PALIT, has been carried out under our supervision and that this work has not been submitted elsewhere for a degree.

(G.C. Ray)
Assistant Professor
Electrical Engg. Dept.
I.I.T. Kanpur

(J.L. Batra)
Professor
Industrial and Management Engg. Programme
I.I.T. Kanpur

August, 1990.

ACKNOWLEDGEMENTS

I take this opportunity to express my deep sense of gratitude to Dr. J.L. Batra and Dr. G.C. Ray for their valuable guidance, critical appraisal and constant encouragement throughout the work.

I wish to thank all technical staff of A.C.E.S. and I.M.E. for their cooperation during the course of the experimental work.

I am highly indebted to my friends, Taranjit Singh and Ms. K. Seshu for their kind help and inspiration.

I would like to thank Mr. U.S. Misra and Mr.J.C. Verma for their excellent typing and drawing respectively.

-BHASKAR PALIT

CONTENTS

Page

LIST OF TABLES

LIST OF SYMBOLS

SNR, S/N	signal to noise ratio
Na^+	sodium ion
K^+	potassium ion
AP	action potential
SEMG	surface electromyogram
h(t)	mathematical expression of single motor unit
MU	motor unit
Hz	unit of frequency
N	Newton
F	force
Ω	Ohms
db	deci bell
M bytes	mega bytes
Σ	summation
μ	mean
σ	standard deviation
ρ	correlation coefficient
E[ ]	expected value
$R_x(o)$	autocorrelation
MEC	myoelectric channel
FFT	fast Fourier transform

η	1.1
V_T	threshold voltage
I_o	reverse saturation current
R_i	resistance
V	voltage
ln	logarithm

ABSTRACT

The object of the thesis is to investigate the signal-to-noise ratio of multi-myoelectric processors and to correlate the electromyographic potential with the muscle force for non-isometric contraction of muscles. The electromyographic potential, picked-up by the surface electrode is termed as surface emg. The non-isometric contraction has the usual significance that while exerting a certain force, the muscle length changes. Experimentally, the relationship between surface emg and muscular force has been found to be nonlinear. The correlations between SEMG and muscular force can be used to determine muscular force by measuring surface emg during locomotion. The amount of emg output can be used as a measure of the relative tension in the muscle and from this assessment could be made how load and position affect myogenic spinal joint compression and muscular fatigue. The following two muscles have been studied in detail: "extensor carpi ulnaris","abductor digiti minimi" at different muscle contraction rates.

The subject matter of this work has been presented in five chapters: Chapter 1, gives a brief introduction to general physiology excitable tissue and bioelectric phenomena. The effect ofstimulus to cause excitation and muscular contraction are discussed in brief. Finally, the problem is outlined and formulated.

The experimental set-up for the measurement of force and emg at different muscular contraction rates have been described in Chapter 2. It includes surface electrodes, multi-EMG channels, a force recorder set-up, multi-channel recorder, a FFT analyser and GPIB interface enabling data transfer between the FFT analyser and personal computer. The scheme for measurement of force and emg at three different contraction velocities have been discussed.

Chapter 3 deals with a multi-myoelectric channel (multi-MEC) model for improvement of the signal-to-noise ratio (SNR). It is shown that SNR depends on both correlation coefficient and number of channel used. The channel performance analysis is carried out for correlated multi-MEC. A time delay technique for SNR improvement has also been studied. In both cases it is found that SNR of multi-MEC is more than SNR of signal pick-up by single channel.

In Chapter 4, both analog and digital techniques to linearize integrated surface emg (ISEMG) have been discussed. The transfer function of black box in which ISEMG is input and the output which approximates the muscular force has been found out using both analog and digital technique.

Finally scope of further work has been discussed in Chapter 5.

CHAPTER - 1

INTRODUCTION AND FORMULATION OF THE PROBLEM

1.1 ELECTRICAL IMPULSES IN HUMAN BODY AND ITS TRANSMISSION

1.1.1 Introduction

Electromyography is concerned with electric phenomena occurring in the muscular tissues and its reaction to electrical stimuli. Electromyography requires the knowledge of electrophysiology of living tissues, bio-electric phenomena associated with them and a sound knowledge of electrical instrumentation and signal processing.

Historically, the presence of electricity in living organism was detected as early as in the times of Galvani and Volta around 1790. By using a simple galvanometer, Mattsucci showed in 1838 that the muscle exterior was electrically positive to muscle interior. He also proved that the potential difference of the state of rest declined sharply during excitation. He further proved that if a second nerve was brought in contact with a contracted muscle, it lead to the contraction of the second also. It can then easily be inferred that the potential generated due to contraction of the first muscle is strong enough to stimulate the nerve in contact.

1.1.2 Resting Membrane Potential and its Origin

A potential difference of 60-90 millivolts exists between the outer surface of axon and its inner protoplasm. This potential difference is called the resting membrane potential. The surface is positive with respect to the protoplasm.

The chemical composition of fluid inside the nerve cell is different from the fluid outside the semipermeable cell membrane. The inner fluid contains a lower concentration of sodium and chloride ions and a higher concentration of potassium ions. These differences in concentration of ions would cause a diffusion across the membrane. The membrane does not permit a free passage of ions. The cell contains a high concentration of protein anions which cannot diffuse through the membrane into the fluid outside, where the concentration of protein is low. Because electric charges of opposite sign attract each other, the protein anions inside the cell attract cations which can permeate through the cell membrane. The membrane is much less permeable to Na^+ than to K^+. The tendency for K^+ to diffuse out of the cell according to a difference in concentration gradient is counteracted by the attraction from the protein anions inside the cell. As long as the Cl^- is in diffusional equilibrium, the outward flux of K^+ is slightly larger than the inward flux and the inward flux of Na^+ is many times greater than the ourward flux. Hence, there must be

a forced movement of Na^+ outward and K^+ inward to balance the diffusion. The net effect of this different distribution of ions on the two sides of the cell membrane is a higher concentration of anions in the interior of axon. A potential difference of about 70 mV according to Nerst equation is present over the membrane, the interior being negative with respect to the exterior. A disturbance of the resting potential difference would occur if the Na^+ and K^+ ions were allowed to move according to the diffusion gradients. An inward flow of positive ions Na^+ would decrease the potential and cause a hypopolarization and an outward flow of K^+ ions would give rise to hyper polarization as shown in Fig. 1.1.

1.1.3 Action Potential and its Origin

All axons can pass from a state of physiological rest to one of excitation in response to a stimulus. The nerve and muscle tissues, which give rise to an electrical impulse, travelling along the membrane in respect to a stimulus, are called excitable tissues. If an electric current of sufficient magnitude and duration is passed through the living tissue it gets excited and it shows in the form of rapid variation of the membrane potential. This potential is called action potential. Above a certain threshold combination of magnitude and duration of the injected current pulse, the nature of action potential

waveform does not change as shown in Fig. 1.2. In the figure it is clear that the potential rises from -70 mV to + 30 mV and falls back to -70 mV indicating a temporal change in the inner surface membrane's potential from being negative to positive with respect to outer surface. The initial polarization of the membrane vanishes in the ascending phase of the action potential, it is called depolarisation phase and the descending phase is called repolarization phase. The duration of action potential may vary from 0.2 to .5 milli-sec. in the axon.

A precondition for the appearance of an action - potential is critical depolarisation of the membrane. During indirect stimulation the critical depolarisation of the membrane is affected by the acetylcholine secreted in the nerve endings upon arrival of a nerve impulse. The action potential generated in the region of the myoneural junction is transmitted further along whole muscle fibre. During direct stimulation by an electric current the action potential (AP) in the muscle fibre arises at the cathode and spreads from there throughout the fibre. The AP lasts for 2 to 5 milli-sec, that is to say, five to ten times longer than that of the motor nerve fibres supplying it.

A potential difference develops across the cell membrane due to presence of concentration gradient of ions. Action potential is generated because of the change in permeability of the membrane due to the stimuli applied. With no stimuli, the cell membrane is more permeable to potassium than to sodium. As a result there is a greater flow of positively charged potassium ions from the protoplasm to the extracellular fluid than the reverse flow of sodium cations, hence the outer side of the membrane is electrically positive w.r.t. inner surface.

When stimulus is applied the membrane permeability for the sodium ions becomes ten times that of potassium ions. As a result the flow of sodium ions into the cell exceeds the outflow of potassium ions out of the cell, thus reversing the sign of membrane potential. This is called depolarisation phase. However, the increased permeability to sodium ions is short lived and a restorative process begins soon. The sodium permeability of the membrane falls. This phase is called inactivation and repolarisation takes place.

1.1.4 Propogation of Action Potential

Action potential arising in an excited cell becomes a stimuli for the adjoining cells and causing sympathetic

excitation in adjoining cells. Since the magnitude of action potential is larger than the threshold of stimulation, an undamped wave of excitation travels all along the excitable tissue.

The mechanism of conduction of excitation from one portion of the fibre to the other portion is same as the generation of action potential. In both the cases when the depolarisation reaches a critical value (the stimulation threshold), an action potential is generated. When current is injected into a part of the excitable tissue, the depolarisation begins at the cathode, an electric current flows between the excited (electronegative) and resting (electropositive) parts of the membrane. The speeds of conduction may be as high as 120 metres per second. The mechanism is shown in Fig. 1.3.

1.2 ACTION POTENTIAL PICKED UP BY BIPOLAR ELECTRODE

Let h(t) be the mathematical expression of single motor unit (will be explained subsequently) action potential as shown in Fig. 1.4. A specific form that provided a reasonable fit as given by Shenedy Ketal [1]

$$h(t) = K\, t\, e^{-at} (2 - at)$$

where a and K are constants.

The temporal pattern of this action potential, as represented by h(t) will look different if it is picked up

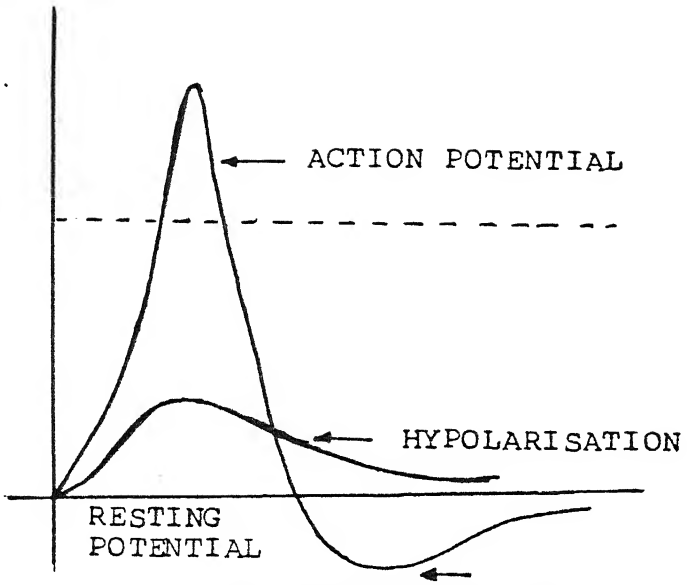

FIG. 1.1

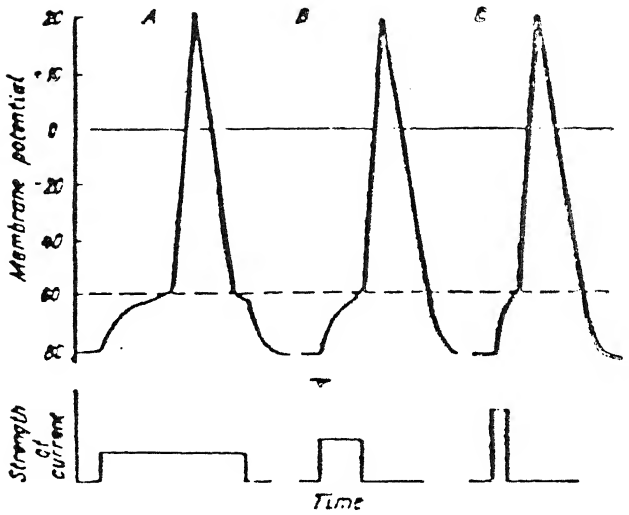

FIG. 1.2

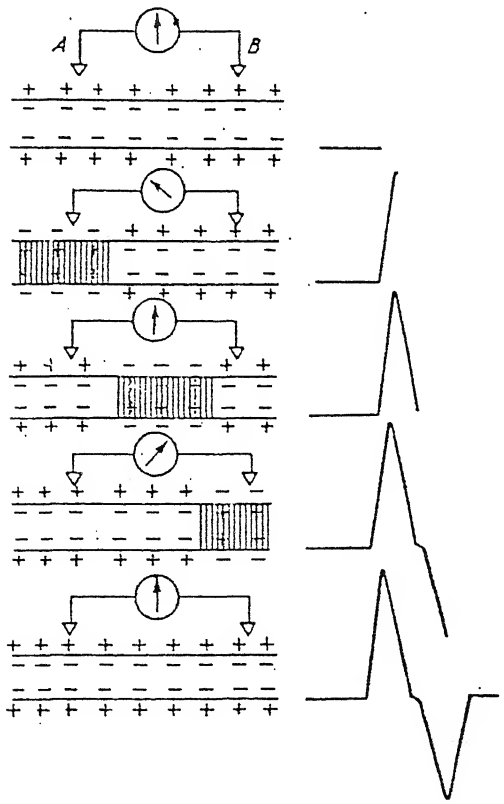

FIG.1.4

.1.3 : MECHANISM OF DIPHASIC ACTION POTENTIAL GENERATOR

by a bipolar electrode. Due to the attenuation in the magnitude, let $h_1(t)$ be the AP picked up by the first electrode with respect to the ground electrode as shown in Fig. 1.5. Since the other electrode is at a different distance, the AP picked up by it with respect to same ground electrode is represented by $h_2(t)$. The bipolar electrode is connected to a differential amplifier, whose output is the difference $h_1(t) - h_2(t)$. The AP picked up by bipolar electrode will have both the positive and negative peaks as shown in Fig. 1.6.

1.3 THE EFFECTS OF CURRENTS ON LIVING TISSUES

1.3.1 The Laws of Stimulation

The electric current is an important agent which can give stimulus to muscle tissue if it is below a certain critical value above which the tissue damage occurs. The effect of this stimulus is quickly reversible. An electric current may be applied with the help of extracellular or intracellular electrodes, the latter being more accurate because it prevents branching of current.

For a stimulus to cause excitation it must have necessary strength, sufficient duration and steepness. The lowest strength of stimulation which can give rise to an action potential is called threshold of stimulation. A stimulus below it is called subthreshold and above it is

superthreshold. The threshold of stimulation is liable to change depending upon physiological condition of the tissue and method of stimulation.

The minimum duration for which an electric current must be applied to a tissue to cause an excitation is inversely proportional to its strength. In Fig. 1.7, it is shown that a current below a minimum strength does not cause excitation irrespective of the duration of application. This minimum current is called rheobase. The time for which a current equal to rheobase must be applied to cause excitation is called utilisation time which implies that further prolongation of the current does not effect the excitation. If the current is increased, the time needed for excitation reduces, however, this time must be above a certain minimum time. It has been observed that rheobase slightly fluctuates depending upon different physiological states of rest.

The threshold of stimulation depends on the duration of stimulus and the steepness of rise as well. If the excitation is induced by a rectangular pulse, the threshold of stimulation is minimum. The threshold of stimulation varies inversely with respect to steepness. If the steepness is less than a minimum no action potential develops, no matter how great is the final current strength. This

happens because if the rate of increase is slow, active changes take place inside the tissue for sufficient time so as to raise the threshold of stimulation. This phenomenan of adaptation of excitable tissue to a slowly increasing stimulus is known as accommodation as shown in Fig. 1.8.

1.3.2 Effect of Direct Current on Living Tissue

A direct current polarises the tissue. A peculiar characteristic of living tissue is that on application of direct current, the excitation arises at the cathode when the circuit is made and at the anode when the circuit is broken. Also, the threshold of excitation at the moment of opening the current circuit is considerably higher than its closing.

The passage of electric current through a living tissue produces changes in the membrane charge. The region where the anode is placed, the positive charge on the outside of the membrane increases causing hyperpolarisation and vice-versa. In both the cases of increase and decrease of current, the excitation builds up and then ceases exponentially. This exponential drop is due to the capacitive behaviour of surface membrane as shown in Figure 1.9. The outer and inner surfaces of the membrane form the plates and the layer of lipoids form the dielectric of very high strength. The pores in the membrane, which allows ions to flow, makes it a leaky

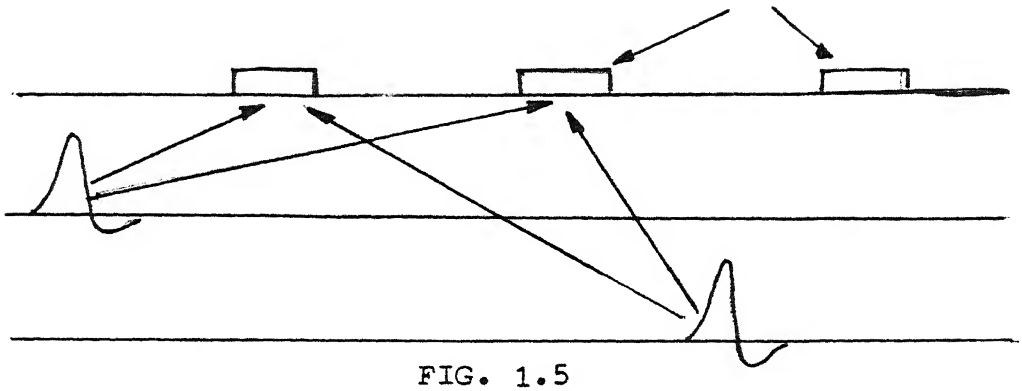

FIG. 1.5

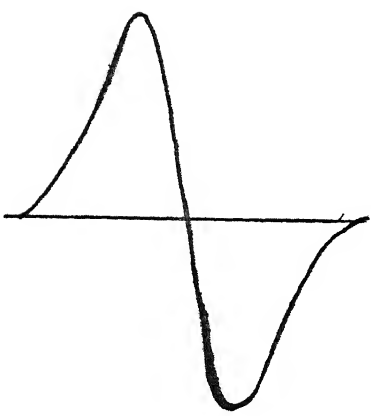

FIG.1.6: ACTION POTENTIAL PICKED UP BIPOLAR ELECTRODE

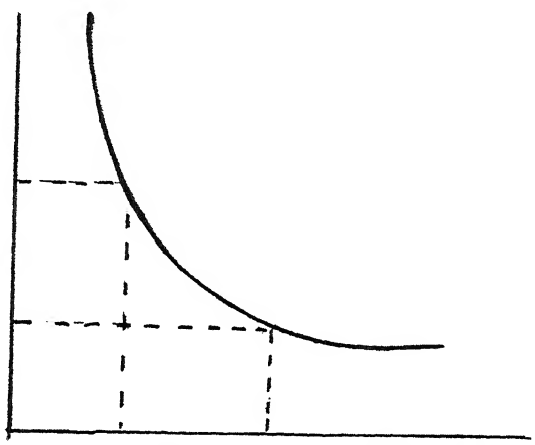

FIG. 1.7 : STRENGTH-DURATION CURVE

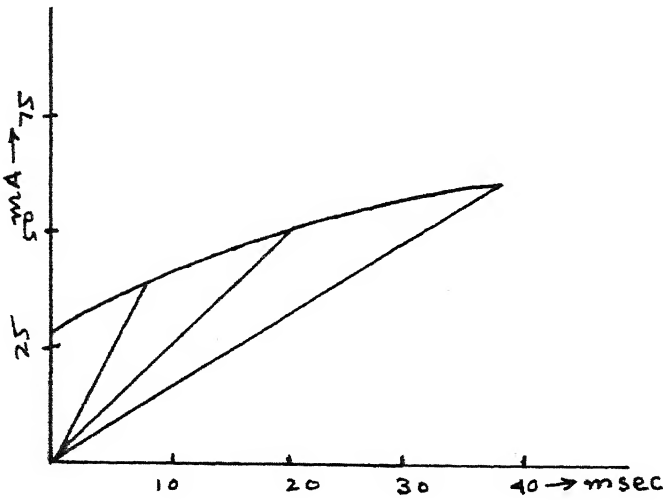

FIG.1.8 : ACCOMMODATION NERVE FIBRE

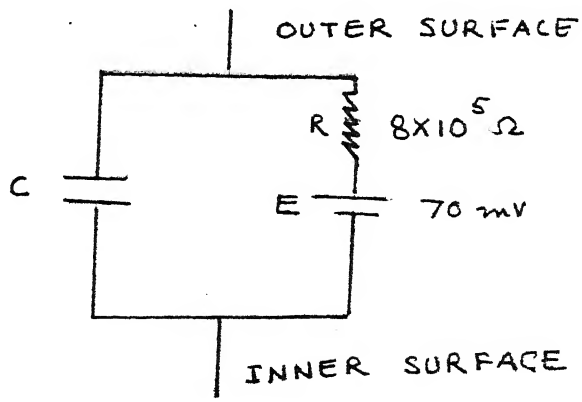

FIG.1.9 : ELECTRICAL PROPERTIES OF A MEMBRANE

capacitor.

The rate of change of membrane potential depends upon the resistance R and capacitance C or the membrane time constant.

A rise in membrane potential at the anode (passive hyperpolarisation) is not accompanied by change in ion permeability even when a strong stimulus is applied. This is the reason why no excitation occurs at the anode when a d.c. circuit is closed. On the other hand a fall in membrane potential near the cathode (passive depolarisation) first causes a brief increase in permeability to sodium ions and then a slow increase in permeability to potassium ions as shown in Fig. 1.10.

The sodium permeability starts rising when the current reaches 50 to 80% of the threshold and rises further till action potential appears. The increase in sodium permeability does not peak immediately. First of all, the depolarisation of the membrane at the cathode causes a relatively slight increase in sodium permeability. Then as the positively charged sodium ions begin to enter the protoplasm, depolarisation of the membrane increases, leading to consequent considerable rise in sodium permeability and hence further depolarisation which again increases sodium permeability. This is called regenerative depolarisation.

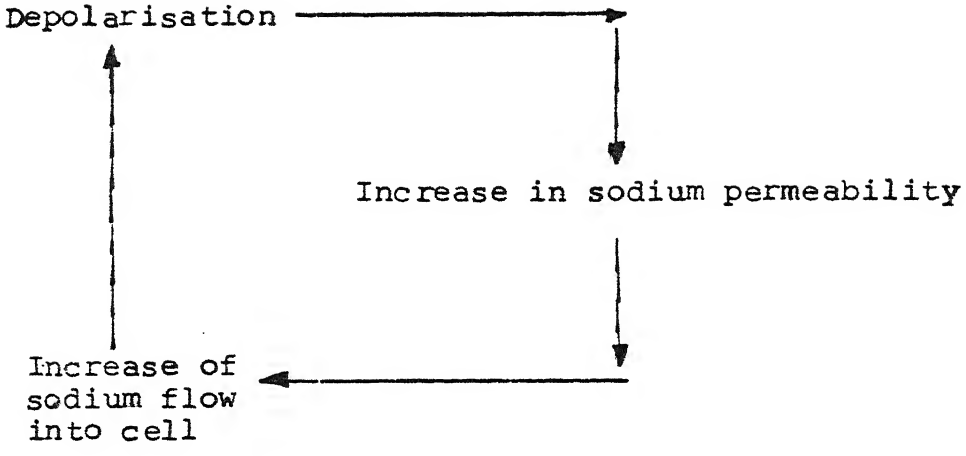

It is believed that the pores through which sodium ions can diffuse into the cell are plugged in a state of rest by calcium ions (being larger in size) and these calcium ions pass out of the pores when the depolarisation occurs in response to a stimulus and thus makes way for the sodium ions.

The sodium permeability remains increased only for 1/10th of a milli-sec and then it starts reducing. This cannot be raised again by active depolarisation due to the property of inactivation. This inactivation of sodium permeability ultimately leads to triggering of the repolarisation stage.

1.3.3 All or None Law

This law states that a subthreshold stimulation produces no excitation while threshold stimuli produce maximum excitation immediately and is unaffected by a

further increase in stimulus strength. The merely states that either no single muscle fibre is excited or all of them get excited together.

1.4 MUSCLE CONTRACTION

The striped skeletal muscles consists of fibres varying in length from a few millimeters to several centimetres and from 10 microns to 100 microns in diameter. Each fibre is a multinuclear structure. The fibre is enveloped in a transparent sheath, the sarcolema, which appears under microscope to be structureless.

These fibres do not exert a constant contractile force, but rather contract and relax repeatedly at rates as high as 35 times/sec. The fibres are innervated in groups. Each group, which contain from 2 to 2000 fibres depending upon the muscle function is innervated by a single nerve axon. The group of fibres together with the axon and the nerve cell body is referred to as motor unit (MU) [4] and is considered the basic functional unit of a muscle.

Contraction of a muscle can be induced experimentally by stimulation. Excitation of the muscle using external electric current stimulus is known as direct stimulation. Stimulation of a motor nerve, leading to contraction of the muscle is called indirect stimulation. The extent of an isolated contraction of skeletal muscle varies with the strength of the stimulation. With threshold strength, the

contraction is barely noticeable but increases with an increase in the strength of stimulus (submaximum contraction). Above a certain strength of stimulus, contraction remains unchanged (maximum contraction).

In natural conditions a skeletal muscle motor unit usually receives from the nervous system a number of nerbe impulses in rapid succession. The rate at which these impulses are received by the motor unit is called firing frequency. Under the influence of this rhythmic stimulation an intense and continuous contraction of muscle occurs, known as tetanic contraction. The tetanic contraction of a muscle considerably exceeds the maximum amplitude of an isolated contraction. Fig.1.11 illustrates the fact that each excitation in the process of rhythmic stimulation causes an additional contraction which is summated to the previous one.

The nerve axon transmits impulses at very great speed. Hence, the muscle fibres making up a motor unit become excited more or less at the same time. The electrical activity of a motor unit is illustrated by a serrated line in Fig. 1.12, which shows each peak corresponds to the aggregate action potential of many simultaneously excited fibres.

Although the muscle fibres of each motor unit are excited synchronously in response to an efferent impulse,

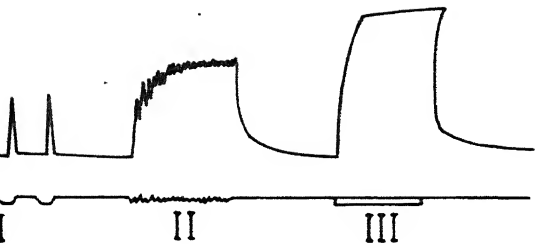

g.1·11 Muscular contractions with muli of different frequency.
frequent stimuli cause isolated ntractions (I); more frequent muli, incomplete tetanus (clonus)
,more frequent still, complete tanus (III)

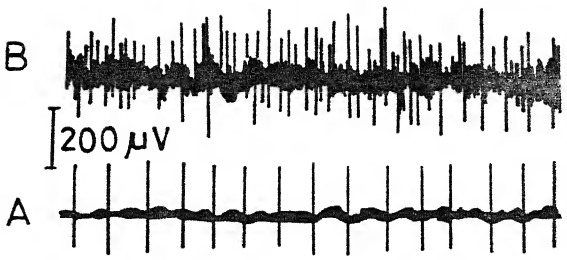

Fig.1·12 Electrical activity of a single motor unit (A) and a whole muscle (B) in man

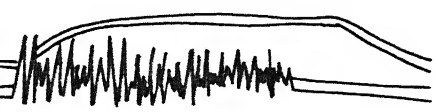

g.1·13 Simultaneous record of tetanic contraction (A) and action currents (B) of muscle

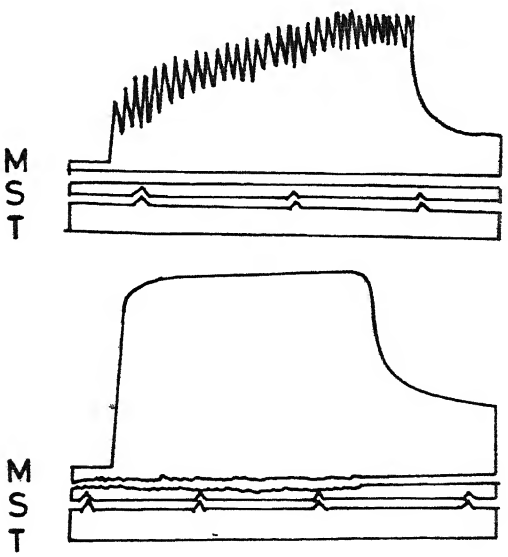

Fig.1·14 Tetanus in an isolated muscle fibre

the fibres of the different motor units of a muscle as a rule function asynchronously [1,2,3,5] because they are innervated by various motor neurons which emit impulses at different frequencies and at different moments. The aggregate contraction of a muscle as a whole is of a combined character under normal conditions and resembles complete tetanus in form even when each of the units function at a slow rhythm. Therefore, by asynchronous activity of the motor units, all movements of the body are smooth even with low-frequency motor impulses. The asynchronous activity of motor units prevent the determination of electrical activity of an individual MU when picked up by unipolar or bipolar electrodes of diameter 3 mm. The signal picked up is a stochastic in nature when picked up from whole muscle as shown in Fig. 1.5.

MU's are having different sizes. All the motor units do not fire together in response to a stimuli. While the force is gradually increased on the body of the muscle more and more MU's come into action [1,2,4,6,7,8,9,10,11,12]. Large MU's fires only if all small motor units have fired 13 . Since different MU's contain different number of fibres the magnitude of AP varies. It has been found tout that peak to peak amplitude of waveform of AP increases with the force. The phenomena of gradual firing of MU's of a muscle is called recruitment and when a MU is first recruited it fires at a fixed

frequency. For example in bicep of a man it is 7 impulses/ sec. A MU which is active increases its firing frequency by 1.4 Hz/N [3] . If for example we take a force level of 20 N, the firing frequency of this motor unit will become (7 + 1.4x20) 35 Hz. This will give rise to 35 Hz component in the EMG signal.

The number of additional motor units recruited during a given increment in force declined sharply at high level of voluntary force [2]. The approximate relationship is

$$(\Delta N) = a\, e^{-bT_i} = a\, e^{-b\, K_1 F}$$

where ΔN = number of newly recruited motor units at the force level F for an incremental change of force (F) and a,b are constants [4]. This suggests that even though the high threshold units generate more contraction, the contribution of recruitment to the increase in voluntary force declines at high force levels [4] .

When the force level increases, the rate of discharge of a motor unit, already active, is increased. This is called rate coding. Peak to peak amplitude of the waveform contributed to the surface emg by a motor unit increases near linearly with the threshold force[2] in case of isometric contraction (explain in Section 1.5.1)

$$2A = K_1 F \qquad (1)$$

where A = amplitude of action potential. F is threshold force.

From equation (1) it is evident that there is a significant tendency of the units recruited with larger force to contribute a greater voltage to surface emg. If the rate coding is neglected, all the MU's of a particular muscle will fire at the same frequency at all force level. This will lead to a variation in the surface emg proportional to the square root of muscular force. But rate coding makes it linear [4,14,15,16].

As the force level is increased, more and more synchronization among the motor units is obtained [17,18]. Due to the effect of synchronization, the action potential of a particular motor unit is effected by the electric fields produced by all the surrounding motor units. The resulting disturbances of electric potential in and near the muscles are very complex because the electromagnetic field is continuously changing with respect to time and position. When plotted as a function of time, they constitutes the familiar interference pattern of electromyography as shown in Fig. 1.15 .

1.5 EMG - MUSCLE ACTIVITY CORRELATION

When a muscle contracts, two parameters are easily measurable. One of the parameter is the force of contraction and the other is the integrated electrical activity. The first one can be measured by a suitable transducer and the second parameter can be processed through

a EMG-channel and can be recorded. The correlation between these two parameters can, then, be obtained experimentally and this result may be used further for better understanding of the physiological mechanism of muscular contraction.

At present, it is generally agreed that the increased force of muscular contraction is obtained by recruiting more motor units and also by increasing the firing rates of the motor units already active [1,2,4,6,7,8,9,10,11] . When a muscle contracts normally, the force of contraction also depends on the change of length of the muscle. Muscles are, elastic and hence it will be reduced in length both the ends are free. The equilibrium length and the resting length are defined as follows [19] .

Equilibrium Length

Unstimulated or resting skeletal muscle is normally under slight tension, since it shortens some what (20%) after its tendons are cut. The length of the unattached, relaxed muscle at which the resting tension is zero is the equilibrium length.

Resting Length

The muscle length at which maximal contraction tension is developed is the resting length. This length has been considered close to the maximal extension possible under normal conditions in the body.

When the tension is developed in the muscle, it may be isometric, nonisometric or isotonic condition. When the tension is developed but the muscle is not allowed to shorten the condition is called isometric contraction. When the tension is developed and the muscle length also changes the condition is called non-isometric contraction. When the muscle is allowed to shorten and it lifts a constant weight, the contraction is called isotonic, since it maintains the same tension during the whole process of lifting.

1.5.1 Isometric Contraction

When force of contraction is developed in muscle, it can be measured experimentally. This measured force will be equal to the force of contraction provided the contraction occurs in isometric condition. Experimental evidences in case of isometric contraction were obtained in early fifties that the integrated electrical activity is having a near linear relationship with the muscular force [20] . Bigland and Lippold [20] measured the integrated electrical activity for the various parameters of the muscle. The latter was subjected to increase and decrease of length at different velocities, or the velocities were changed for the same tension or same length of the muscle. In every case near linear relationship was obtained though the slope of the lines were different.

Mathematical model which can justify the linear relationship in case of isometric contraction are available [1,21,22, 23]. Theoretical studies by many authors have attempted to establish this linear relationship owing to its importance in practical application such as the proportional control of the gripping force of a prosthetic hand or in tactile feedback. Most of these studies suggest that the amplitude of the EMG should increase as the square-root of the tension rather than linearly, if motor units fire independently of one another.

1.5.2 Non-Isometric Contraction

If change in length of the muscle is allowed, a passive elastic tension is developed in the muscle which is to be subtracted from the total measured force to obtain the force of contraction developed in the muscle. This is explained with the help of Fig.1.16 and Fig.1.17 . When an unstimulated skeletal muscle is stretched the passive elastic tension increases as an exponential function of length over a length upto 200% of the equilibrium length as shown in Fig. 1.16 (in the figure, 100 represents the equilibrium length, resting length is about 125) [19]. Stretches upto atleast 150% of equilibrium length are perfectly reversible, the muscle snaps back to its equilibrium length when released. Skeletal muscle ruptures at about three times its equilibrium length. Figure 1.17 shows the relation between tension developed during maximal voluntary effort and the

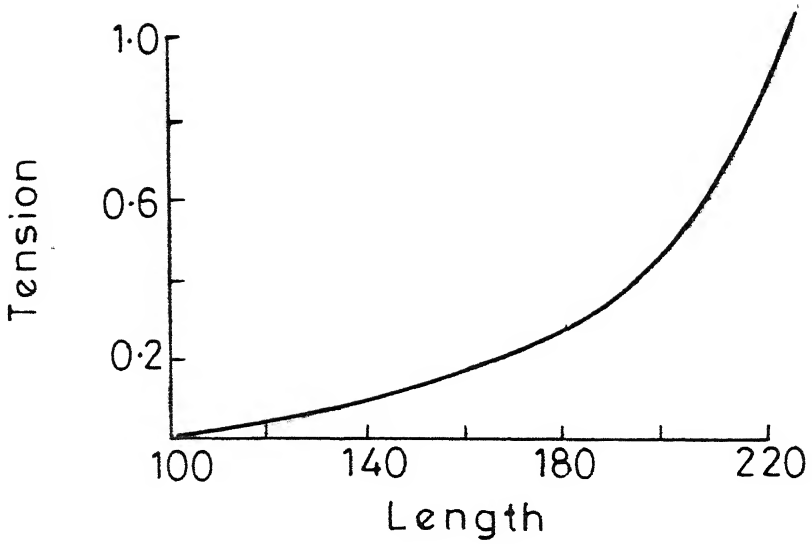

FIG·1·16 STATIC LENGTH TENSION DIAGRAM OF ISOLATED SKELETAL FIBRE AT REST

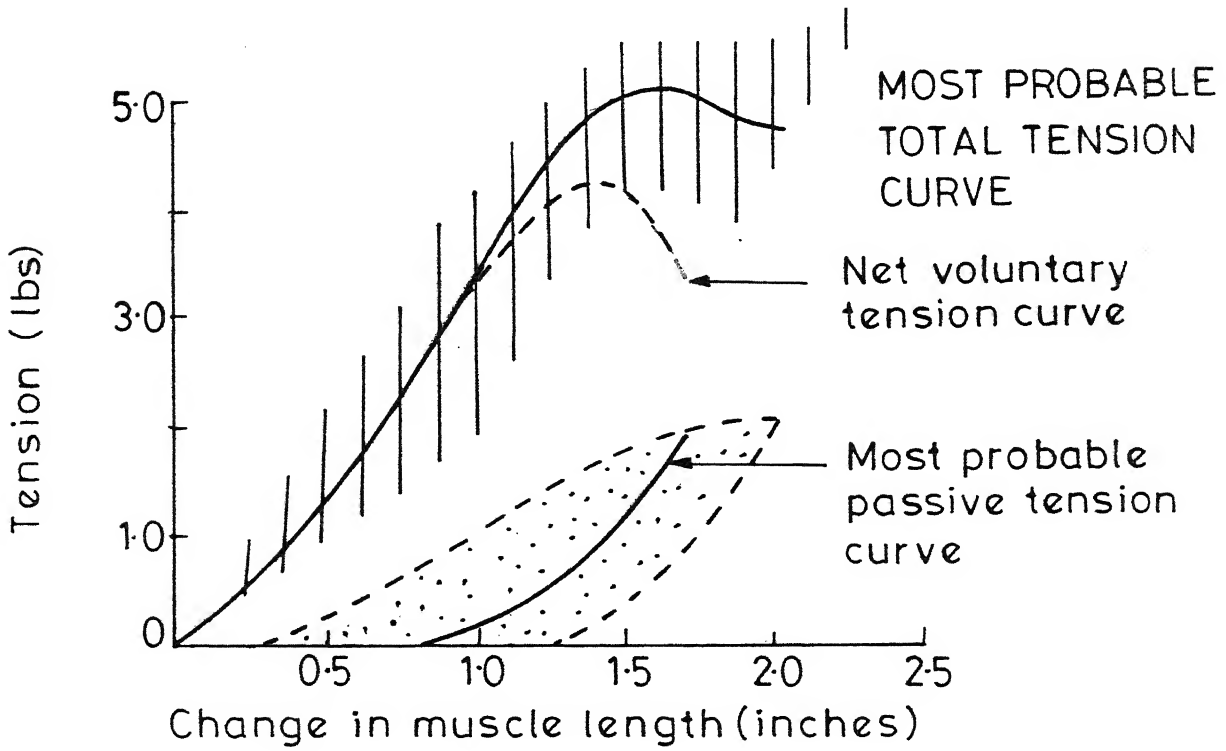

FIG·1·17 ISOMETRIC LENGTH TENSION SUMMARY FOR HUMAN TRICEPS MUSCLE

length of the triceps muscle in man. The net or active voluntary tension curve is obtained by stretching the muscle fibres and connective tissues to any given length and then subtracting the value obtained from the total tension exerted by the contracting muscle at the same time.

It is obvious from these two figures that the force of contraction of a muscle is more difficult to calculate if the muscle is subjected to change in length. For involve testing of the muscles the experimentation is more complicated and the precise knowledge of anatomy is needed.

1.6 FORMULATION OF PRESENT PROBLEM

A general background is given in the previous part of this chapter with emphasis on recent developments. In light of this the following problems have been identified and formulated for the present work.

It is difficult to provide a mathematical model correlating the surface emg with muscular force in case of non-isometric contraction because it is difficult to take into account the passive elastic tension developed in the muscle and also to determine it experimentally. So, one of the objective of the present work is to give a transfer function relationship between the integrated EMG as input and force measured by transducer as output. The detailed experimental arrangement is given in Chapter-2.

The EMG picked up by surface electrode in the case of non-isometric contraction depends upon

(1) The length of muscle

(2) The choice of muscle

(3) The location of electrodes

(4) Temporal pattern of emg picked up by electrode.

1.6.1 The Choice of Muscle

On the entire human body there are hardly a few joints which are controlled by single muscle. In most of the cases, several muscles are involved for sending joint. In such a case, the amount of force exerted by muscle is difficult to know without precise knowledge of anatomy of all the muscles involved.

In the present analysis the muscle, "extensor carpi ulneris" and "abductor digiti minimi" were selected for study. The muscle "extensor carpi ulneris" was more or less solely responsible for wrist abduction. Except for a little contribution (about 20%) by"fluxor carpi ulneris", other muscle contribute hardly anything for this movement. The muscle "abductor digiti minimi" which is a small muscle, responsible for the abduction of little finger was selected. For abduction of more than 2 mm (more than 1 cm in present study) the length of the muscle is changing, so the condition is non-isometric construction of muscle.

1.6.2 The Length of Muscle

A small muscle is having larger number of small motor units and fewer number of large motor units e.g. eyelid muscle, muscle in forearm where as a big muscle has small number of small MU and large number of large MU e.g. back muscle, thigh muscle. So in the case of small muscle the incremental force is small for each newly recruited motor unit. So, it is possible to get small incremental force in case of small muscle as shown in Fig.1.18.

1.6.3 Location of Electrodes

Surface electrodes used to pick up emg have a diameter of 3 mm. Hence, these electrodes pick up emg only from a small area around the electrode. When independent output from adjacent muscles or from closely spaced areas in one muscle are required, spatial selectivity may be a problem. An finally a fundamental limitation of all surface electrode systems, regardless of design is that only superficial muscles can be used. The action potential picked up by electrodes depends upon the depth of muscle fibre. The maximum height corresponds to the action potential coming from the muscle fibre nearest to the skin. Similarly, the minimum one is coming from the muscle fibre lying in the deeper layer. The variation is given by

$$\frac{E_r}{E_o} = \exp(-0.2\, r \sqrt{f_o})$$

r = depth of muscle studied in cm

f_o = mid-band frequency of EMG spectra

E_r = potential difference observed at distance r, radially from the fibre

E_o = potential difference at the fibre.

When EMG interference pattern is picked up by the surface-electrode, the action potential of motor units lying near the skin will contribute more high frequency components. Motor units lying at deeper layer will contribute less high frequency components as shown in Fig. 1.19.

1.6.4 Temporal Nature of Action Potential

The action potential picked up by bipolar electrode has both positive and negative peaks, superimposed on it the noise signal [24] . The amount of noise present in normally processed EMG output is relatively large. This noise increases in magnitude with increasing contraction level.

The most commonly used technique for SNR enhancement of myoelectric channel is by applying an averaging filter. It is clear that the averaging filter in the ME channel can only increase SNR at the cost of an increase in response time. However, in a myoelectric control system or other applications the time is an important

factor and sufficient averaging to achieve a high SNR may be prohibited. So, in order to enhance the performance signal processing time must be small. So, the effect of multimyoelectric channel on SNR improvement is analyzed under the assumption that the signals from N channels are uncorrelated. This is under the assumption that the signal from one channel is distinct from other channel electrodes. At closer distances, these N channel signals become correlated due to the fact that the some common motor units may be picked up by different channels. A model to account for the correlation between signals in the multi-channel case and detailed experimental results are discussed in Chapter-3.

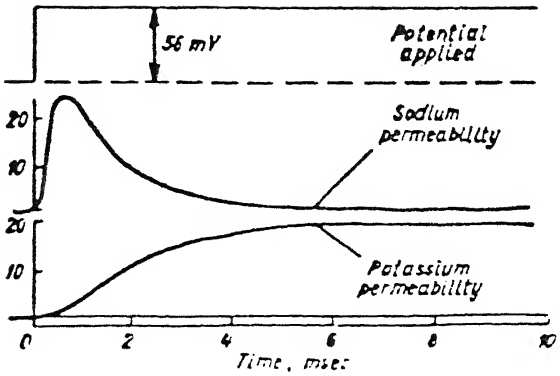

Changes in sodium and potassium permeability of a membrane during depolarisation by a direct current

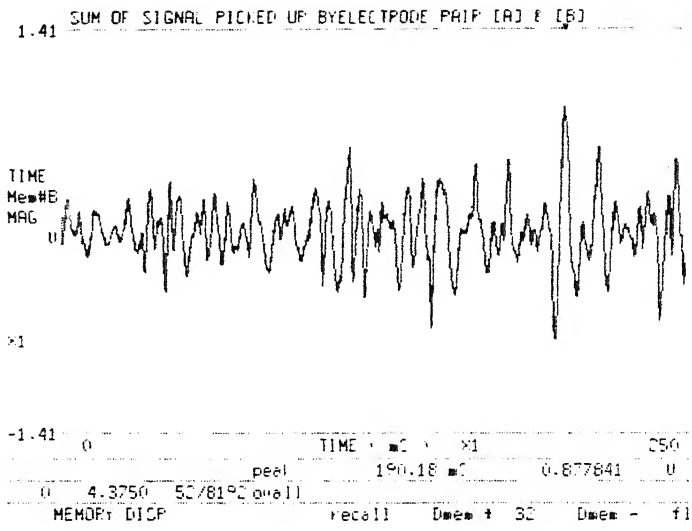

FIG. 1.15

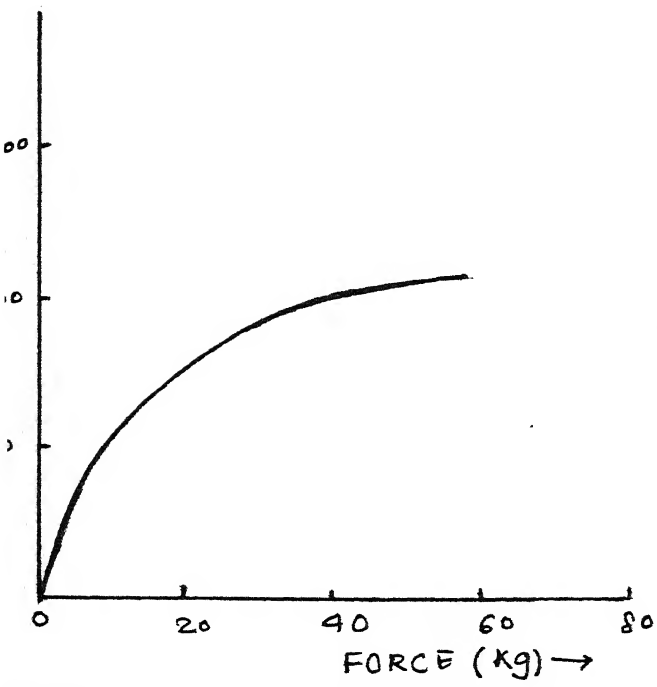

1.18 : NUMBER OF MU RECRUITED FOR DIFFERENT LEVEL OF TOTAL MUSCLE FORCE

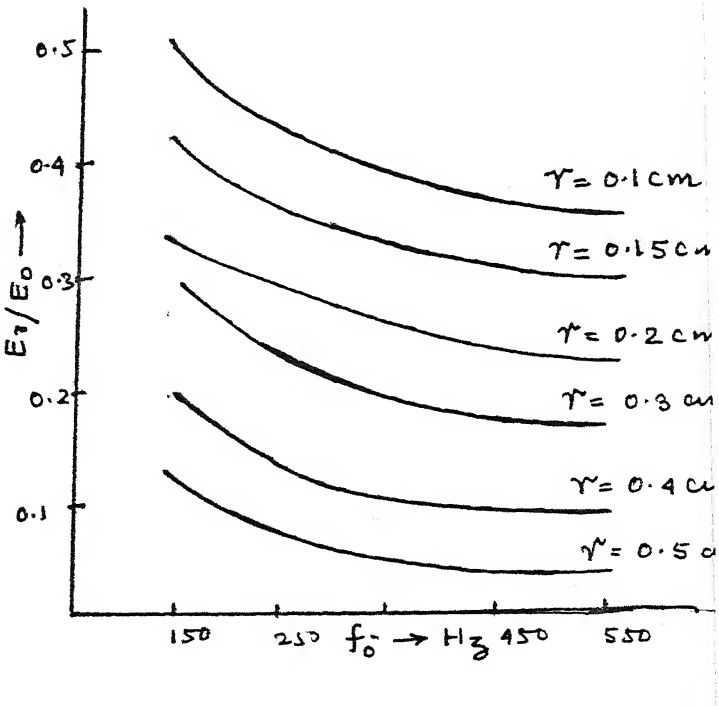

FIG. 1.19 : R.N. SCOTT'S FORMULA

CHAPTER - 2

THE EXPERIMENTAL SET-UP

2.1 INTRODUCTION

The science of recording electrical phenomena which accompanies muscular activity is known as electromyography. This can be recorded using surface electrodes or using micro-electrodes which can be injected into the muscle. In order to extract the EMG signals which are deeply immersed in noise and are relatively weak signals, it is required to do some sort of S/N ratio enhancement. When a muscle contracts two parameters are easily measurable, the force of contraction and integrated electrical activity.

2.2 THE EMG ELECTRODES

The EMG electrodes are meant to pick up the myoelectric signals which are in the microvolt-millivolt range. Since the signals are of low magnitudes, extra care needs to be exercised in the preparation of the electrodes. Different types of electrodes are used in electrophyisology depending upon the requirements for accuracy, reproductibility of results etc. Generally metal electrodes like wires and plates of silver, platinum, nickel etc. are used. These electrodes have low resistances. But it is not recommended to use them for long stimulations since ions from the electrodes pass into the tissue under the action of current

and may have toxic effect. Also while recording d.c. potential, there is a chance of polarisation of these electrodes due to formation of electrochemical cells.

Silver was chosen as the electrode materials since it offers the best performance to cost ratio. Silver with an outer layer of silver chloride is best for electrode material. Each active electrode was 3 mm in diameter while the neutral electrode was 10 mm in diameter. The silver electrode buttons of the two active electrodes were fixed on a plastic base with 1 cm separation.The neutral electrode was fixed separately on a plastic base. This was done to avoid corruption of the signal by low frequency noise due to movement of electrodes while doing physical task. Coaxial cables of smallest available core diameter were chosen to transmit the signals picked up by the electrodes in order to minimise the external noise entering into the system.

2.3 THE EMG CHANNEL

The signals picked up from the surface of the skin have to be processed in several stages before operating a control unit. The maximum r.m.s. voltage obtained between two skin electrode plate of about 1 cm separation is between 50 to 1000 μV. To obtain an output d.c. signal within a dynamic range of a few volts, the required gain from r.m.s. to d.c. must be of the order of 60 to 90 db. The noise signals appearing at both electrodes under identical phase

and amplitude conditions must be suppressed efficiently in order to reduce disturbances. The suppression is obtained by a high CMRR and a high input impedance in the first differential stage. The CMRR should be more than 70 db and input impedance should be more than 100 mega-Ohms. The interface impedance between tissue and electrodes may fluctuate quite considerably. If the input impedance of the amplifier is not high compared to the interface impedance, the fluctuations will cause troublesome errors when common mode signals occur.

The EMG channel is primarily used to differentially amplify the input signals and filter the frequency regions of interest. The EMG channel used consisted of

(1) the differential amplifier
(2) the band pass filter
(3) the adjustable gain amplifier
(4) the half wave rectifier
(5) the full wave rectifier
(6) the low pass filter.

The block diagram of the EMG channel is shown in Fig.2.1 and its electronic circuit realization is shown in Fig. 2.2.

The differential amplifier was incorporated in the circuit to give noise free signals. The high CMRR was accomplished utilizing a potentiometer in the differential

stage. To avoid problems arising from polarisation voltages and the late a.c. coupling, the voltage gain of the differential stage has been kept low. The differential amplifier used three inputs from the three surface electrodes (one reference and two active ones). It amplified only the signals from two active electrodes based on the potential difference between each of them and the reference electrode. Since any interference from external causes produced identical changes in the potentials of all the three electrodes, the output signal was unaffected by external noise.

In the following two stages, the myoelectric signal was amplified and passed to a band pass filter. A resonant type band pass filter was used, lower cut-off frequency being 110 Hz and higher cut-off 280 Hz.

The variable gain amplifier was incorporated to vary the gain to desired level to prevent saturation of the signal.

The half wave rectifier was incorporated to clip off the negative portion of signal. The half wave rectified output was used to analyse the frequency characteristics of the EMG spectrum.

The full wave rectifier and subsequent low pass filter having time constant of 100 milli-sec. was used to reduce ripple to a negligible value.

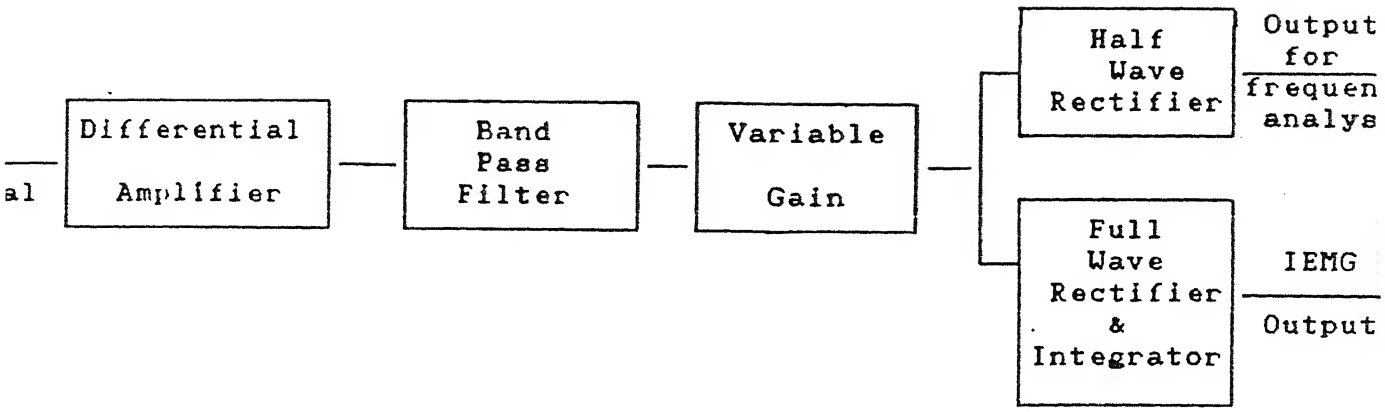

1.1. The block diagram of the EMG channel.

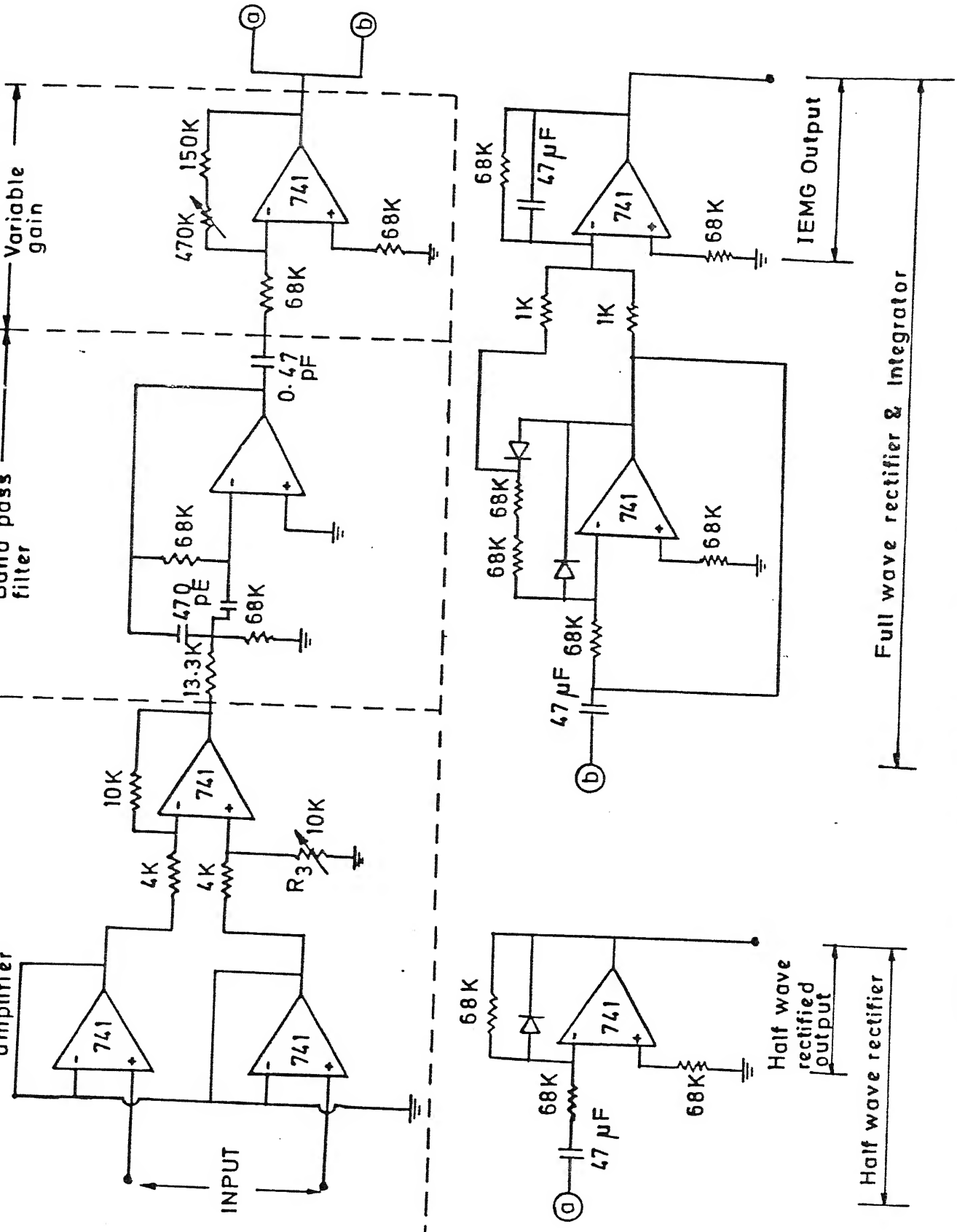

FIG. 2.2 : CIRCUIT DIAGRAM OF THE EMG CHANNEL

2.4 THE FORCE RECORDER

The arrangement for the measurement of force is shown in Fig. 2.3. Two strain gauges (300 Ohms,) used in the wheatstone bridge configuration, as shown in Fig. 2.4. were mounted on two sides of a thin steel-strip. Since the mass of the steel-strip was small, its frequency response is high which permits the measurement of force at high muscular contraction rates. The present study is on non-isometric contraction of muscle and hence the bending of the strip was limited upto 0.8 to 1 cm. For this configuration of wheatstone bridge, the sensitivity of the system gets doubled. This is due to the fact that the bending of steel strip leads to increase in resistance of strain gauge mounted on one side of steel strip and decrease in resistance of strain gauge mounted on other side. This configuration is also insensitive to temperature changes because strain gauges used are identical.

For the configuration shown in Fig. 2.5, even though it is insensitive to temperature change, the sensitivity is half of the configuration as shown in Fig. 2.4.

The output of the wheatstone bridge was made to pass through differential amplifier to remove the effect of noise signal present in the mechanical part of the setup. The zero adjustment of the bridge was achieved with the help of differential amplifier and summing amplifier as shown in Fig. 2.4. When the wheatstone bridge is unbalanced

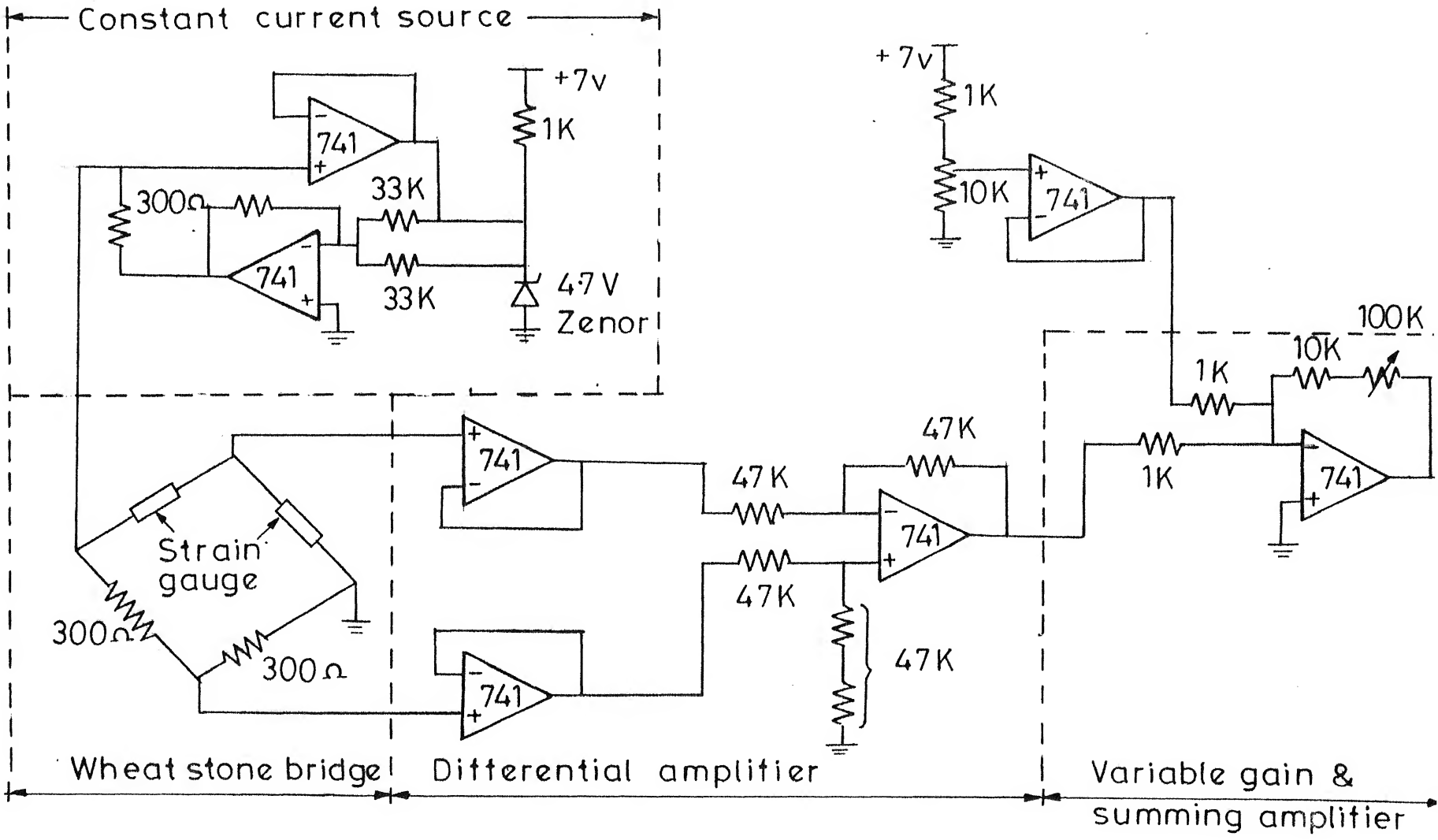

FIG. 2·4 CIRCUIT DIAGRAM OF FORCE RECORDER

Tape Speed	Frequency response
9.52	DC ~ 1.25 KHz
4.76.	DC ~ 625 Hz
2.18	DC ~ 313 Hz
1.19	DC ~ 116 Hz

TABLE 2.1 : FREQUENCY RESPONSE OF THE MULTI-CHANNEL RECORDER AT DIFFERENT TAPE SPEEDS

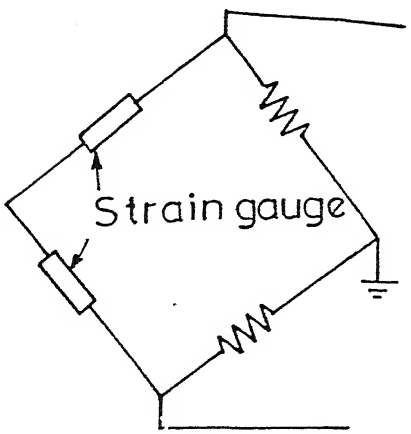

FIG. 2.5

due to bending of steel strip an output voltage appears. Constant current source excitation was used for the wheat-stone bridge so that output unbalanced voltage is also d.c. in nature.

The maximum bending of the steel strip was limited upto 0.8 to 1 cm because the semiconductor strain gauges shows linearity upto that bending limit only. Fig. 2.6 shows the characteristic.

The force recorder was calibrated by applying known forces and output voltages were measured. The calibration curve is drawn, as shown in Fig. 2.7. The characteristic in Fig. 2.7 shows that good linearity is obtained upto 1000 gm of force.

2.5 THE MULTI-CHANNEL RECORDER

The multi channel recorder used in the present set-up was a Tech - MR - 40 model which can record and reproduce 4 channel analog signals on cassette tape. The principle features of this recorder are:

1. 4 tape speeds, 4.8 cm/s, 2.4 cm/s, 1.9 cm/s, 1.2 cm/s
2. channel monitoring
3. an accurate electronic tape counter with LED display.
4. identification code recording, reproduction and search.

The main specifications of the multichannel recorder are

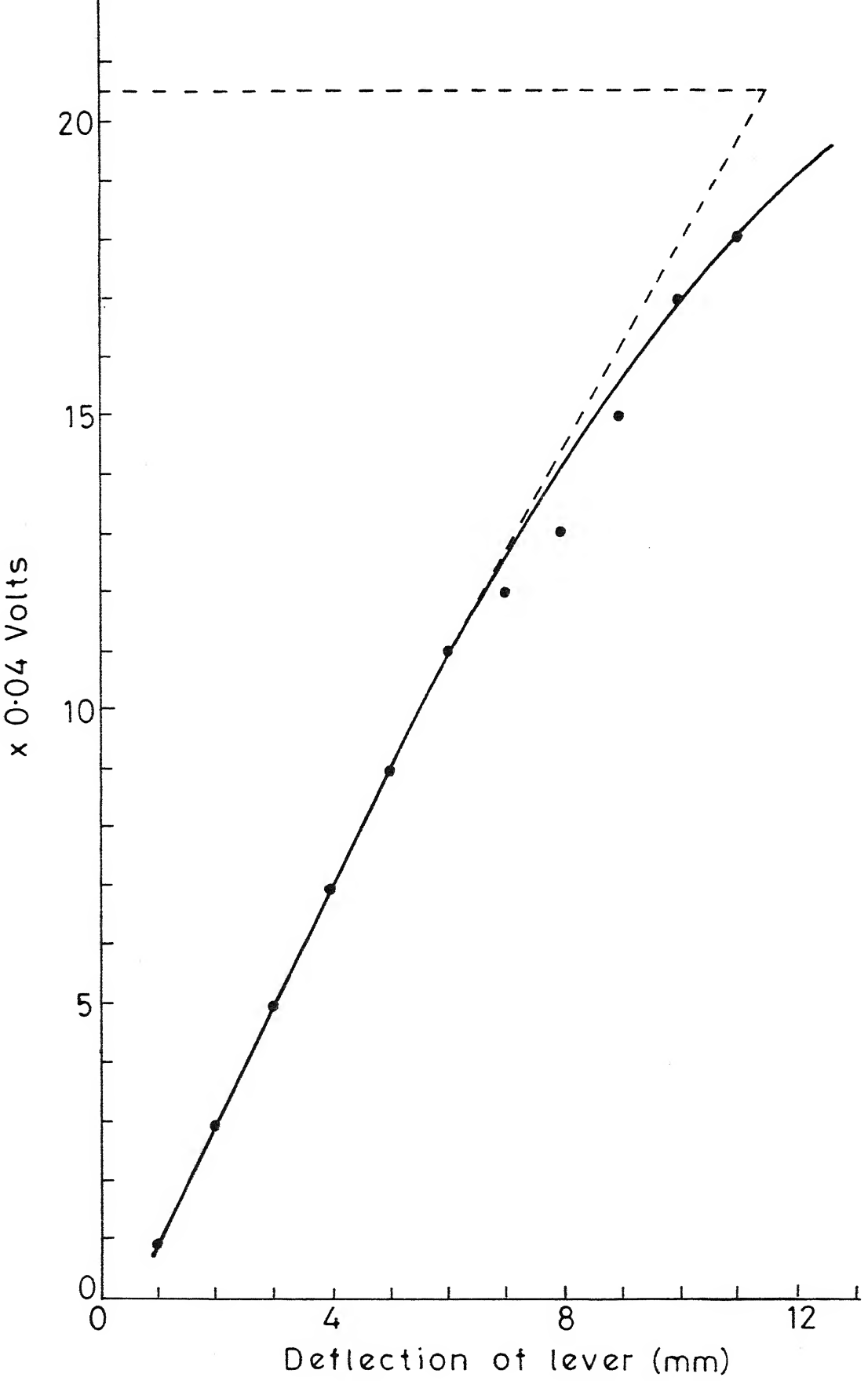

FIG. 2·6 STRAIN GAUGE CHARECTERISTIC

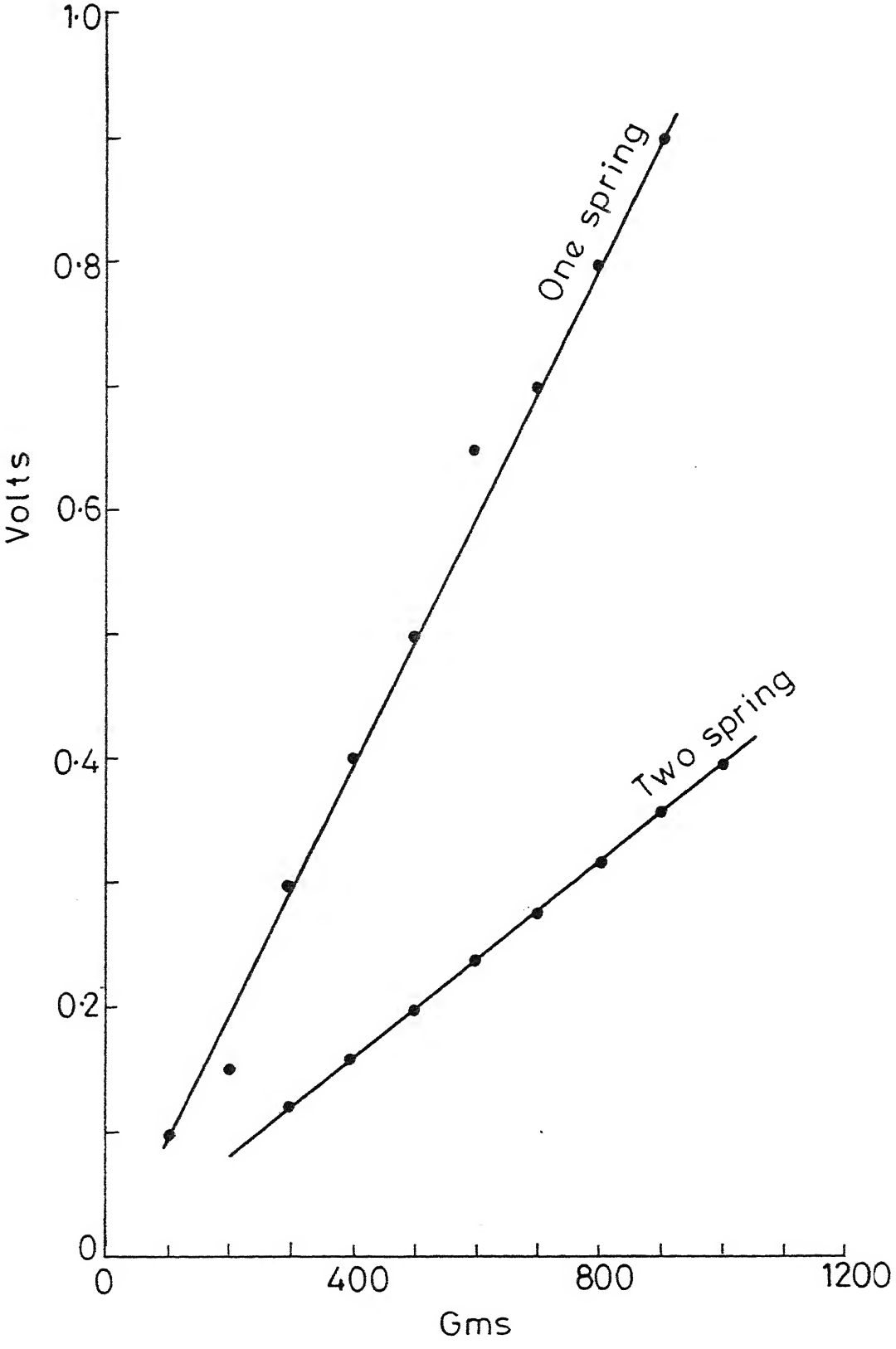

FIG. 2·7 CALIBRATION OF FORCE RECORDER

given below:

Input impedance - 1 M Ohm

Output impedance - 75 Ohm

Output current - 10 mA.

The frequency response of the multichannel recorder at different tape speed is shown in Table 2.1. A tape speed of 4.76 cm/sec. was chosen since the frequency of response was sufficient for truthfully recording the EMG signal.

2.6 THE FFT ANALYSER

The AD-3521 is a two channel FFT spectrum analyser capable of very high accuracy. It has a frequency range of d.c. to 100 KHz, a 15 bit A/D convertor and a full 90 db dynamic range. Both input channels are isolated to allow two signals of differing voltage levels to be analysed at the same time. The following functions are present:

Spectrum	Transfer function
Histogram	Impulse response
Time-waveform	Coherence function
Auto-correlation	Coherence output power
Cross-correlation	Cross-spectrum.

The AD-3521 FFT analyser has a basic memory of 250 Kb. This can be increased to 2M bytes, by the addition of option boards, allowing long term transient capture for future analysis

Single or dual 5 1/4" floppy disk drives can be connected, as an additional option, giving storage facilities for 64 panel conditions and 64 displays per disk.

The main specifications of FFT analyser is given below:

1)	Sampling points	2048/frame
2)	Sampling frequency	4.096 times frequency range
3)	Frequency range	1 Hz to 100 KHz
4)	Windows	Rectangular, Hanning, Minimum Flat top
5)	Delay between channels	Single frame mode-delay within 1 frame Multiframe mode - delay within the set number of frames. Delay is set in units based on seconds.
6)	Frame mode	
	single frame	One frame (2048 time data item) is input and processed
	Multiframe	Multi frame of data are input. One arbitrarily selected single frame is successively extracted for processing.

The analyser can also be connected to an external computer and print-out facilities can be obtained by connecting a video printer to the appropriate output connector on the rear panel of the instrument.

2.7 THE SCHEME OF EXPERIMENT

The scheme is shown in Fig. 2.8. Bipolar surface electrodes were used to pick up emg signal. Since one of the objective of the present experiment was to study the signal to noise ratio improvement using multimyoelectric channels, so two electrode pairs were mounted for study of "abductor digiti minimi" responsible for finger abduction and three electrode pair for "extenser carpi ulnaris". The emg signals picked up by bipolar electrodes have both positive and negative peaks and superimposed noise. The emg signal picked up by all different electrode pairs were summed up using a summing amplifier. The summed emg and emg picked up by different electrode pairs were recorded for study.

To study the surface emg and muscle force correlation in case of non-isometric contraction, the summed emg was full wave rectified and low pass filtered to get d.c. voltage.

Force was exerted on the lever on which strain-gauges were mounted. The deflection was limited to one cm. for non-isometric contraction of the muscle. With the change of frequency in function generator the first light-spot on the oscilloscope traced saw-tooth wave with different velocities. Force was exerted on the lever in

such a way that the second light spot closely follow the first. In this way surface emg and force were recorded for different muscular contraction rates.

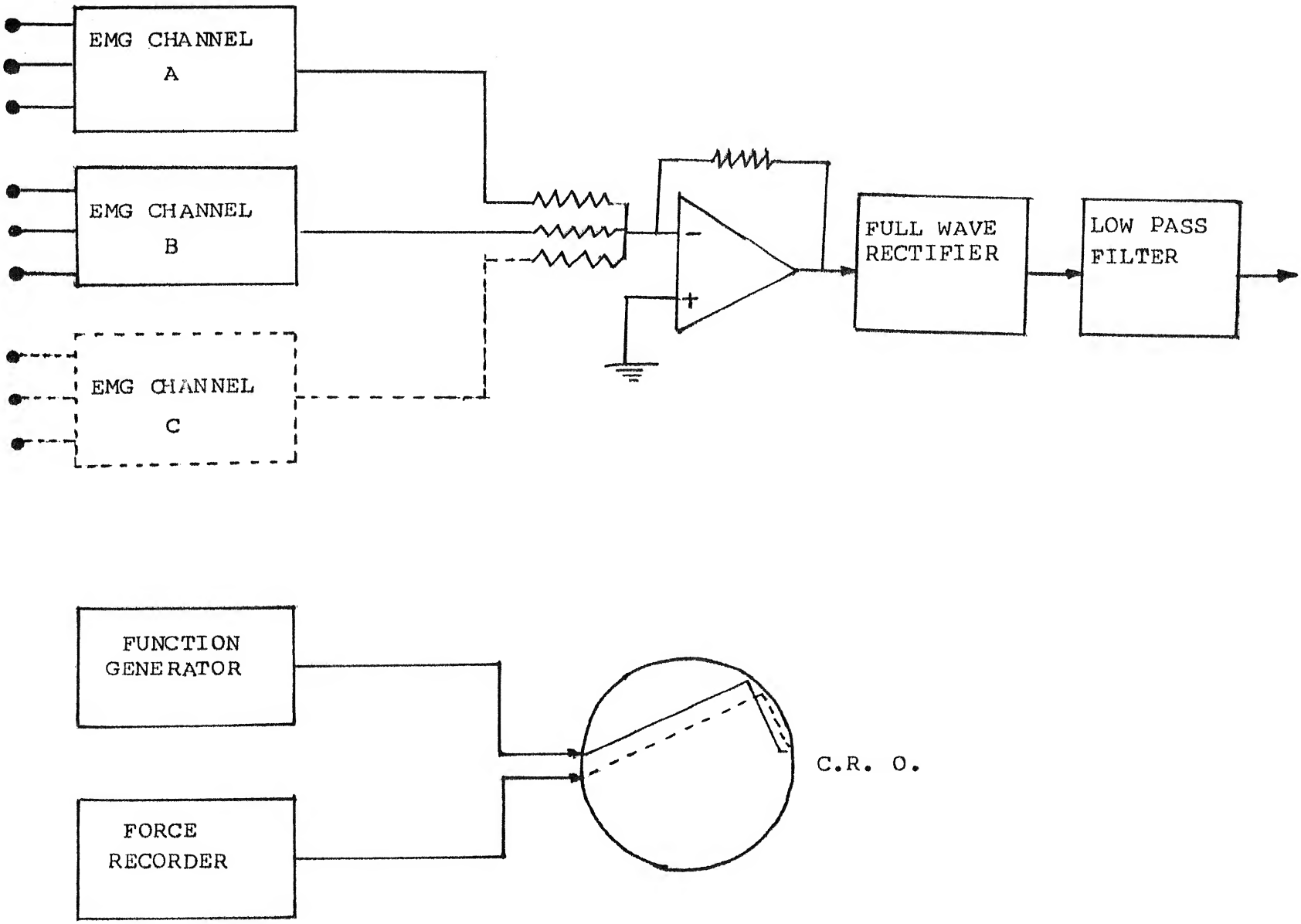

FIG. 2.8 : EXPERIMENTAL ARRANGEMENT

CHAPTER - 3

A SIGNAL-TO-NOISE INVESTIGATION OF A CORRELATED MULTI-MYOELECTRIC CHANNEL

3.1 INTRODUCTION

When surface detected electromyographic activity is to be used for some purpose such as controlling a powered orthotic/prosthetic device, it is often desirable that the control signal derived from the EMG activity be as smooth and responsive to contraction level changes as possible. Surface-detected EMG closely resembles amplitude-modulated random noise and it is necessary that some initial processing be performed to convert this raw EMG activity into a useful signal. Ideal output characteristics of the processed EMG would include a signal monotonically related to instantaneous muscle contraction with no superimposed noise.

A major source of difficulty in proportional EMG control at present is due to relatively large amount of noise present in normally processed EMG output. One desires a processed signal which is a smooth image of the modulating envelope for purpose of correlating electrical and mechanical events. This smoothing can be achieved by low-pass filtering but only at the cost of distortion in the amplitude and phase of modulating envelope which leads

to sluggish system response detrimental to control. Control of sluggish systems is inherently difficult for human because of the temporal lag and distortion in feedback between the user's actuation and system response. Thus the problem is how to obtain a smooth measure of the overall electrical activity of a muscle during both slow and rapid movements without frequency-dependent filter distortion.

There are several methods by which the SNR can be increased.

Method 1: One approach to solving this problem is to use spatial averaging of several uncorrelated EMG signals from a muscle, instead of temporal averaging of a single signal.

Method 2: Using two channels and giving a time delay to signal of one channel and then summing.

3.2 CORRELATED MULTIMYOELECTRIC CHANNEL MODEL

3.2.1 Model

When multimyoelectric channel is used for SNR improvement, it is assumed that the signals from N channels are uncorrelated. This is an approximation of the case where the electrode used for obtaining the signal for one channel is distant from other channel electrodes. At closer distances, these N channel signals become correlated due to the fact that the some common motor units may be picked up by different channels. A model to account for the correlation

between signals in the multi-channel case is discussed below.

The multi - MEC model that accounts for the correlation between channels is shown in Fig. 3.1.

Let $u_{ji}(t)$ $(j = 1,2,....M$ and $i = 1,2....N)$ represent the jth motor units innervation signal in the ith channel. $y_i(t)$ represent the ith myoelectric signal. The mean $E(y_i(t))$ of each channel output is denoted by μ_i and var $\{y_i(t)\}$ by σ_i^2

$$Z = \sum_{i=1}^{N} Y_i$$

$$E\ [\ Z(t)\ ] = E\ [\sum_{i=1}^{N} y_i\ ] = \sum_{i=1}^{N} i \qquad (1)$$

$$E\ [Z^2(t)\ ] = E[\ (\ \sum_{i=1}^{N} y_i(t))^2\ ]$$

$$= \sum_{i=1}^{N} E(\ y_i^2\ (t)) + \sum_{i\neq K}^{N}\sum E(y_i(t)\ y_k(t)) \qquad (2)$$

$$E\ [y_i^2(t)\ ] = \sigma_i^2 + \mu_i^2 \qquad (3)$$

Cross covariance

$$C_{ik} = E\ [\ y_i(t)\ \ y_k(t)\ ] - \mu_i\ \mu_k \qquad (4)$$

Substituting eqns. (3) and (4) in eq. (2)

$$E\ [\ Z^2(t)\ ] = \sum_{i=1}^{N} (\ \sigma_i^2 + \mu_i^2) + \sum_{i\neq k}^{N}\sum (C_{ik} + \mu_i\ \mu_k) \qquad (5)$$

where C_{ik} is covariance between channels i and k.

Cross correlation coefficient

$$\rho_{ik} = \frac{C_{ik}}{\sigma_i \sigma_k} \tag{6}$$

From eq. (5) and eq. (6),

$$E[z^2(t)] = \sum_{i=1}^{N} \sigma_i^2 + \sum_{i=1}^{N} \mu_i^2 + \sum_{i \neq k}^{N} \sigma_i \sigma_k \rho_{ik} + \sum_{i \neq k}^{N} \mu_i \mu_k$$

$$= \sum_{i=1}^{N} \sigma_i^2 + \sum_{i \neq k}^{N} \sigma_i \sigma_k \rho_{ik} + \left(\sum_{i=1}^{N} \mu_i \right)^2 \tag{7}$$

$$\sigma_i^2 = R_x(o) - \mu_i^2$$

$$= E[x^2(t)] - \mu_i^2$$

$R_x(o)$ is autocorrelation at zero.

From eq. (7),

$$\text{Var}[Z(t)] = \sum_{i=1}^{N} \sigma_i^2 + \sum_{i \neq k}^{N} \sigma_i \sigma_k \rho_{ik} \tag{8}$$

From eq. (1) and (8)

$$SNR_{mc} = \frac{\left(\sum_{i=1}^{N} \mu_i \right)}{\left[\sum_{i=1}^{N} \sigma_i^2 + \sum_{i \neq k} \sigma_i \sigma_k \rho_{ik} \right]^{1/2}}$$

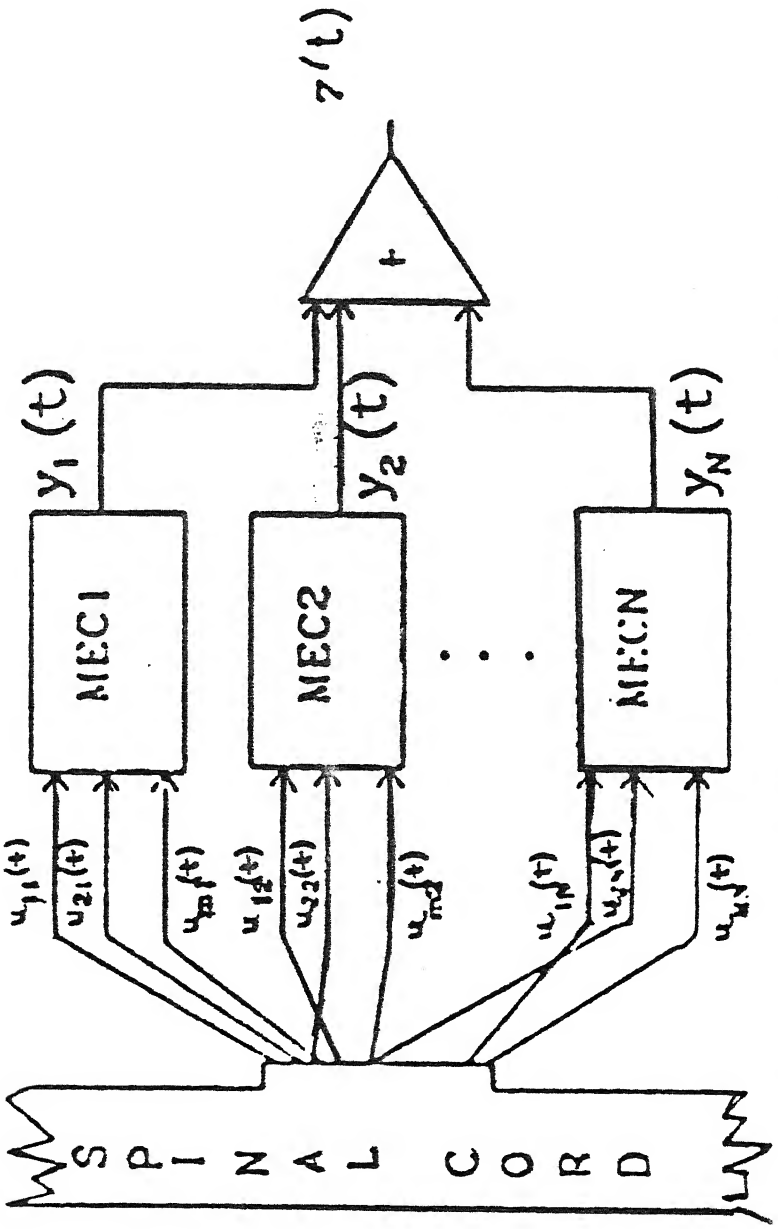

FIG. 3.1 : A Correlated Multi-myoelectric Channel Model, where $u_{mi}(t)$ and $u_{mj}(t)$ are the common units in different channels.

where SNR_{mc} denotes the signal to noise ratio of the correlated multi MEC.

3.2.2 The Experiments

The experiment was conducted on two muscle one small "abductor digiti minimi" and other medium sized muscle "extensor carpi ulnaris." Two channels were used in case of former because it was difficult to place more than two electrodes pairs with sufficient spacing so that emg picked up by the electrode pairs have minimum correlation. Three electrode pairs were placed in case of "extensor carpi ulnaris" with a spacing of 1 cm between two electrode pairs and the ground electrode was placed 3 cm away from the active electrode pairs.

The scheme for recording surface emg picked up by individual electrode pair and their sum for various contraction rates of muscle has been explained in Chapter - 2 under "The scheme of experiment."

The surface emgs recorded were rectified to get substantial mean value of the SEMG and were stored in the memory frame of FFT analyser. The frame to frame analyser was carried out using FFT analyser and various parameters mean, autocorrelation, cross correlation between different channels were calculated. The rectified SEMG picked up by each individual electrode pair, their spectrums, autocorrelations, cross correlation for "extensor carpi ulnaris" are

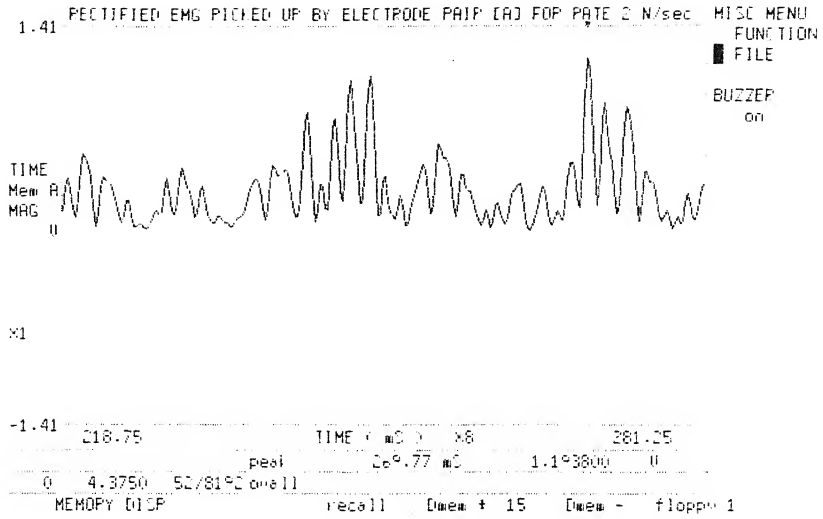

FIG. 3.2 : RECTIFIED EMG PICKED UP BY ELECTRODE PAIR A FOR MUSCLE "EXTENSOR CARPI ULNARIS" WITH MUSCLE CONTRACTION RATE OF 2 N/sec

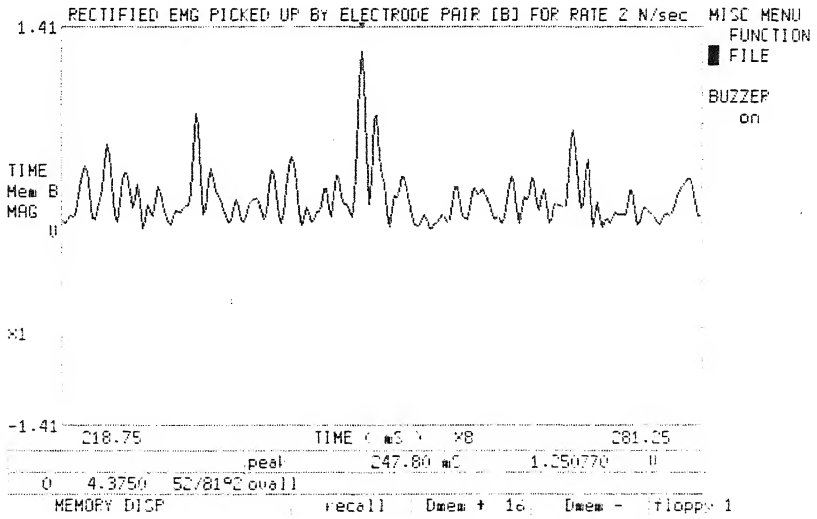

FIG. 3.3 : RECTIFIED EMG PICKED UP BY ELECTRODE PAIR B FOR MUSCLE "EXTENSOR CARPI ULNARIS" WITH MUSCLE CONTRACTION RATE OF 2 N/sec.

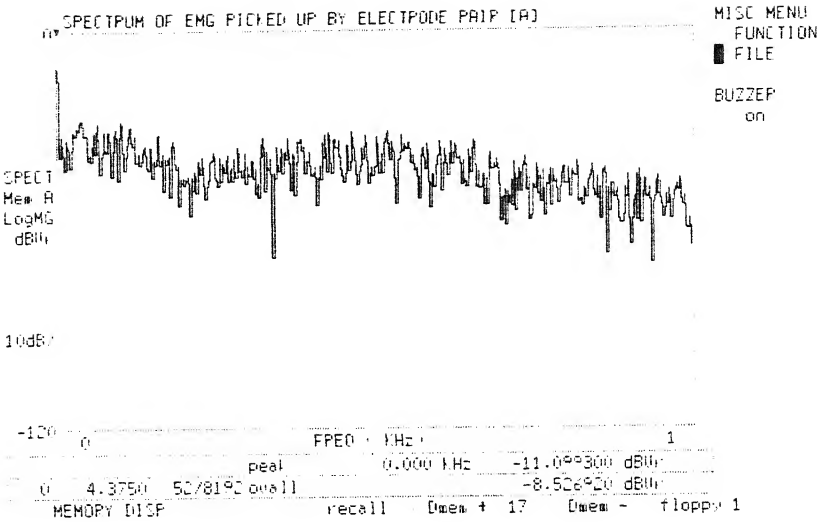

FIG. 3.4 : SPECTRUM OF EMG PICKED UP BY ELECTRODE PAIR A

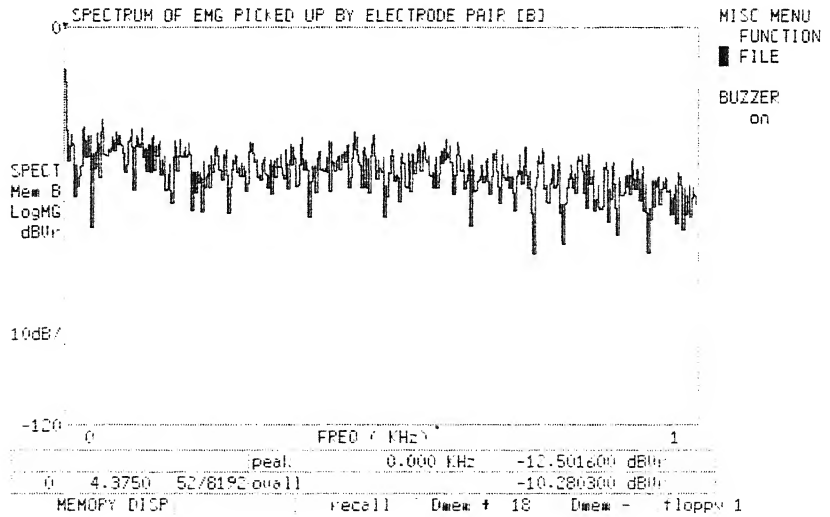

FIG. 3.5 : SPECTRUM OF EMG PICKED UP BY ELECTRODE PAIR B

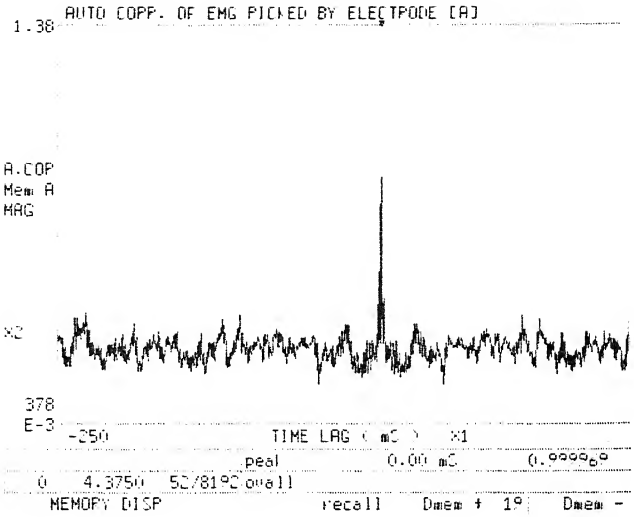

FIG. 3.6 : AUTO CORRELATION OF EMG PICKED UP B
PAIR A

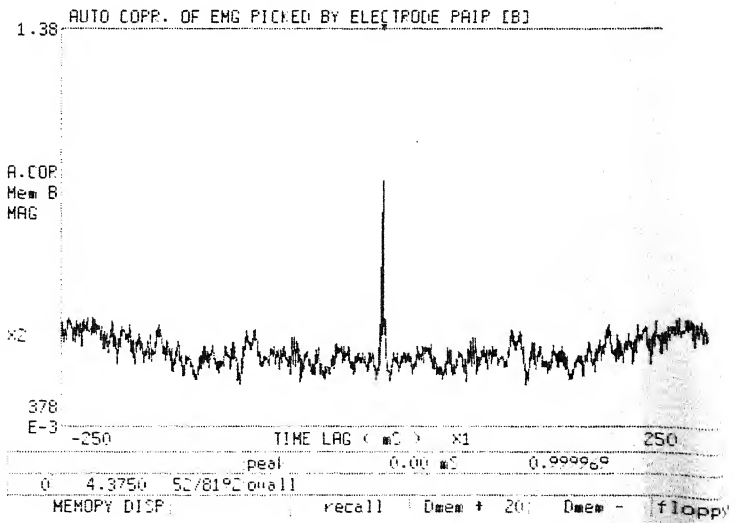

FIG. 3.7 : AUTO CORRELATION OF EMG PICKED UP BY ELE
PAIR B

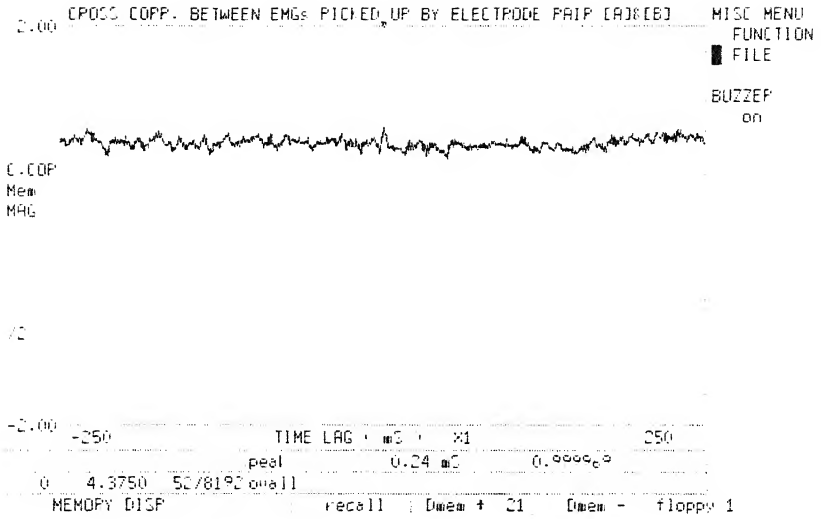

FIG. 3.8 : CROSS CORRELATION BETWEEN EMGs PICKEDUP BY ELECTRODE PAIRS A AND B

shown in Figs. 3.2 to Fig. 3.8.

3.2.3 Results and Discussion

The results obtained from the analysis of the experimental data for SEMG picked up from "abductor digiti minimi" at different contraction rates are shown in Tables 3.1 to 3.3.The variation of SNR of surface emg picked up by each individual electrode and the summed signal with memory frame number are shown in Fig. 3.9 to Fig. 3.18. It is evident from the plot that the SNR of summed signal is higher than the SNR of SEMG picked up by each electrode pair. Also the SNR increases with the memory frame number which is due to the fact that the amount of signal present increases with the increasing contraction (force applied). The variation of SNR with muscular contraction rate is shown in Fig. 3.19 and Fig. 3.20. As the muscle contraction rate is increasing the SNR also increases because with increasing rate of doing work the amount of SEMG present in signal picked up by electrodes increases.

3.3 SNR IMPROVEMENT BY DELAYED SUMMATION

3.3.1 Introduction

The most important component of noise present in surface EMG has frequency of 50 Hz (power line frequency). An improvement in signal to noise ratio can be achieved by time delaying the surface emg picked up by one electrode pair and then summing it with the surface emg picked up by

TABLE 3.1 : Signal to Noise Ratio of SEMG Picked-up from "ABDUCTOR DIGITI MINIMI" for Contraction Rate 0.5 N/sec.

Frame No.	(S/N) of channel A	(S/N) of channel B	(S/N) of summed signal	(S/N) calculated using eqn. 9	Cross-correlation coefficient
1	0.773	0.8546	0.923	0.971	0.277
2	0.6346	0.968	0.981	0.984	0.253
3	0.4732	0.974	1.053	0.993	0.31
4	0.661	0.992	1.174	1.182	0.287
5	0.6445	0.999	1.215	1.199	0.285
6	0.607	1.012	1.261	1.283	0.271
7	0.7195	1.078	1.298	1.274	0.307
8	0.6417	1.095	1.327	1.308	0.317
9	0.7003	1.161	1.394	1.411	0.224
10	0.6686	0.954	1.042	1.134	0.27
11	0.6784	0.992	1.122	1.205	0.286
12	0.7231	1.075	1.173	1.191	0.33
13	0.7324	1.194	1.23	1.256	0.325
14	0.7486	1.213	1.241	1.239	0.276
15	0.7495	1.254	1.256	1.281	0.269

TABLE 3.2 : Signal to Noise Ratio of SEMG Picked-up from "ABDUCTOR DIGITI MINIMI" for Contraction Rate 1 N/sec.

Frame No.	(S/N) of channel A	(S/N) of channel B	(S/N) of summed signal	(S/N) Calculated using eqn. 9	Cross correlation coefficient
1	0.6083	0.874	0.913	0.924	0.219
2	0.748	0.9208	1.071	1.103	0.205
3	0.7489	1.059	1.125	1.171	0.226
4	0.7508	0.9764	1.162	1.183	0.229
5	0.7844	1.083	1.217	1.229	0.218
6	0.8122	1.099	1.251	1.273	0.208
7	0.875	1.103	1.318	1.305	0.198
8	0.881	1.109	1.357	1.381	0.219
9	0.923	1.145	1.394	1.403	0.251
10	0.968	1.187	1.412	1.421	0.233
11	1.023	1.333	1.531	1.507	0.211
12	0.639	0.9284	1.114	1.079	0.270
13	0.732	0.8166	1.108	1.164	0.198
14	0.775	0.9372	1.113	1.129	0.237
15	0.832	0.9966	1.216	1.206	0.215

TABLE 3.3 : Signal to Noise Ratio of SEMG Picked-up from "ABDUCTOR DIGITI MINIMI" for Contraction Rate 2N/sec.

Frame No.	(S/N) of channel A	(S/N) of channel B	(S/N) of summed signal	(S/N) calculated using eq. 9	Cross correlation coefficient
1	0.9955	1.451	1.513	1.575	0.312
2	1.0199	1.456	1.572	1.591	0.367
3	1.018	1.458	1.598	1.601	0.33
4	1.019	1.483	1.627	1.633	0.401
5	0.9007	0.9902	1.073	1.104	0.317
6	1.02	1.157	1.239	1.216	0.324
7	1.021	1.127	1.291	1.273	0.35
8	1.0168	1.356	1.47	1.491	0.305
9	0.9649	1.2879	1.503	1.536	0.331
10	0.9822	1.421	1.548	1.571	0.381
11	0.9937	0.9958	1.109	1.116	0.323
12	0.9984	1.0616	1.175	1.152	0.408
13	0.9999	1.1765	1.265	1.197	0.311
14	1.0144	1.376	1.441	1.425	0.349
15	1.0375	1.394	1.458	1.439	0.332

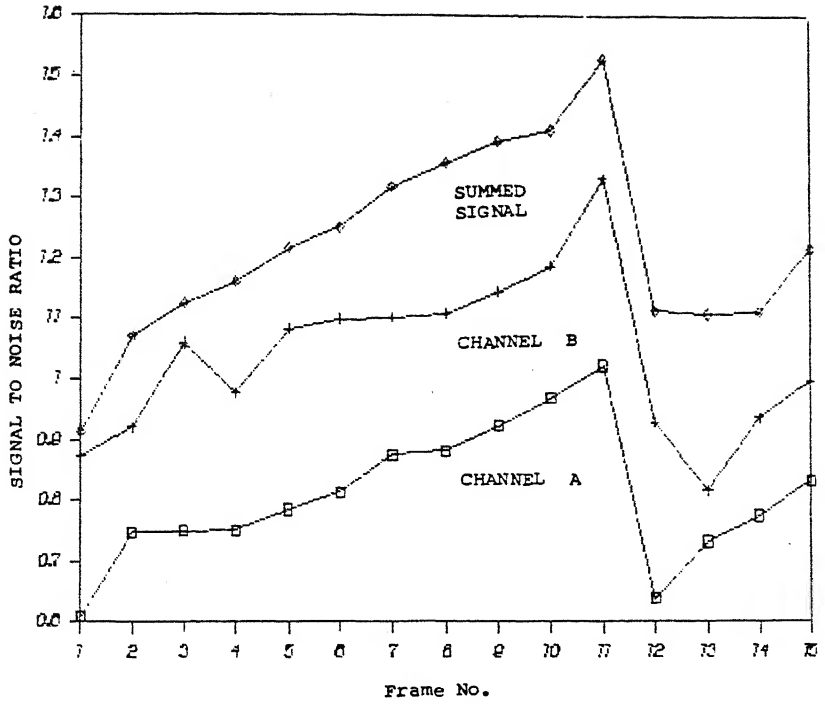

FIG. 3.9 : SIGNAL TO NOISE RATIO OF "ABDUCTOR DIGITI MINIMI" FOR CONTRACTION RATE 1 N/sec.

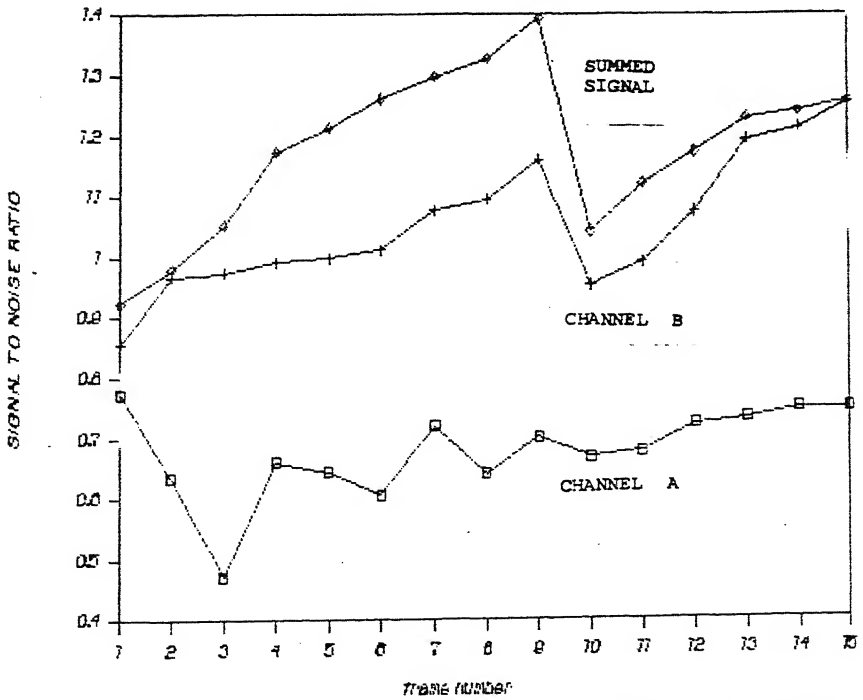

FIG. 3.10 : SIGNAL TO NOISE RATIO OF "ABDUCTOR DIGITI MINIMI" FOR CONTRACTION RATE 0.5 N/sec.

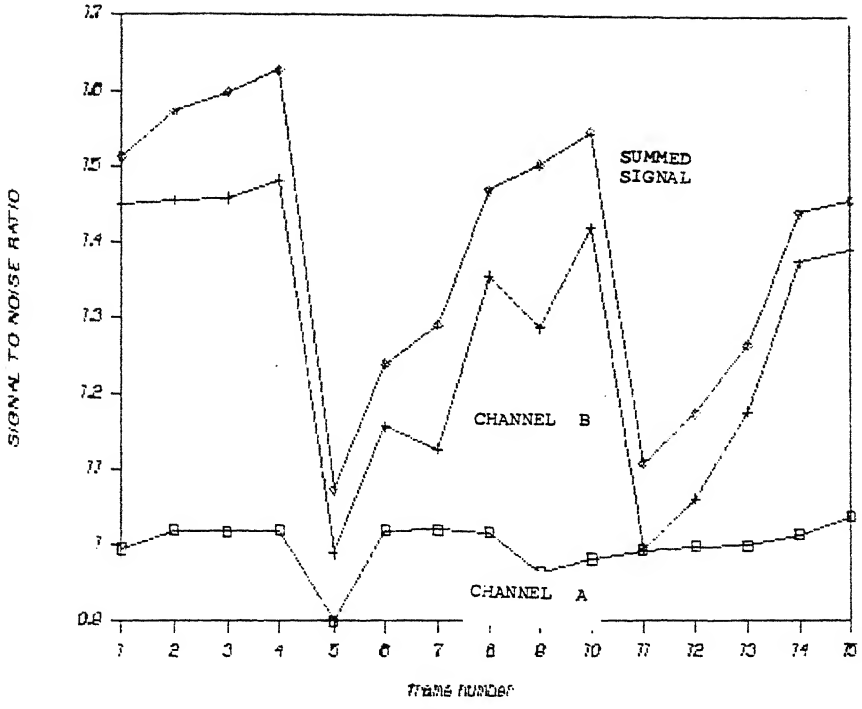

FIG. 3.11 : SIGNAL TO NOISE RATIO OF "ABDUCTOR DIGITI MINIMI" FOR CONTRACTION RATE 2 N/sec.

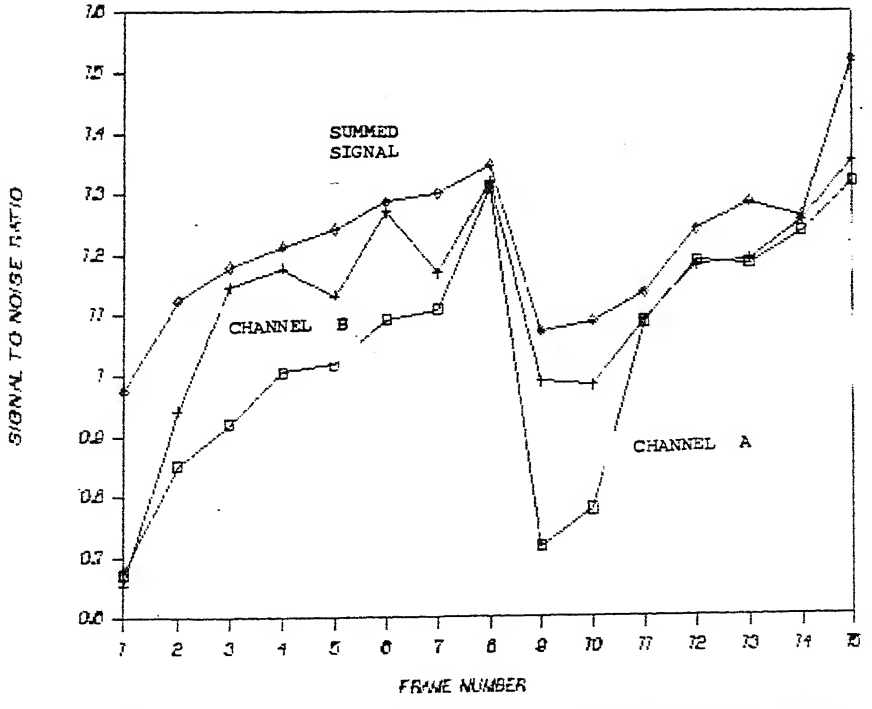

FIG. 3.12 : SIGNAL TO NOISE RATIO OF "EXTENSOR CARPI ULNARIS" FOR CONTRACTION RATE 4 N/sec.

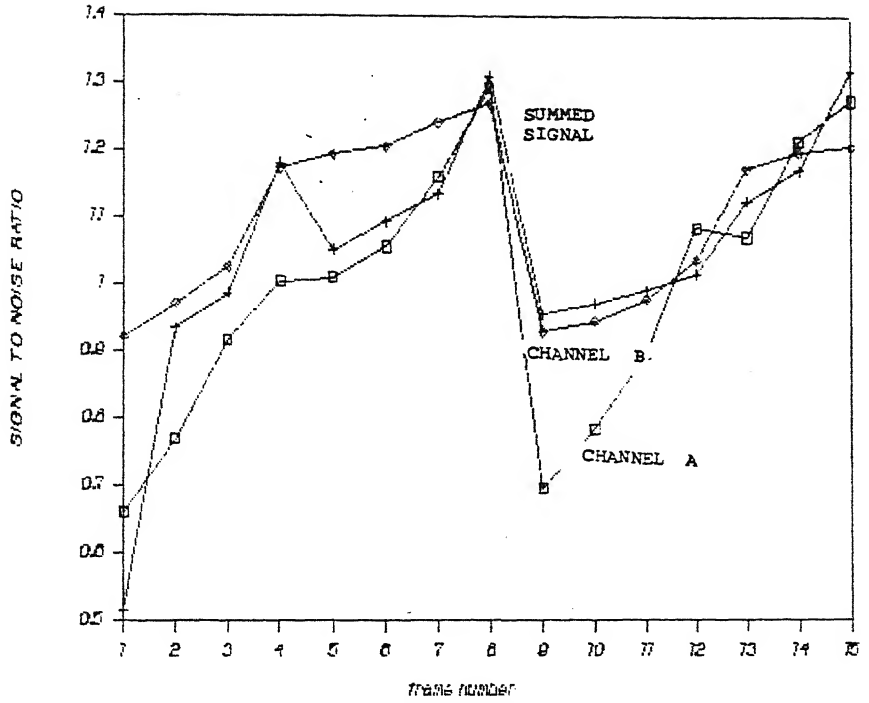

FIG. 3.13 : SIGNAL TO NOISE RATIO OF "EXTENSOR CARPI ULNARIS" FOR CONTRACTION RATE 2 N/sec.

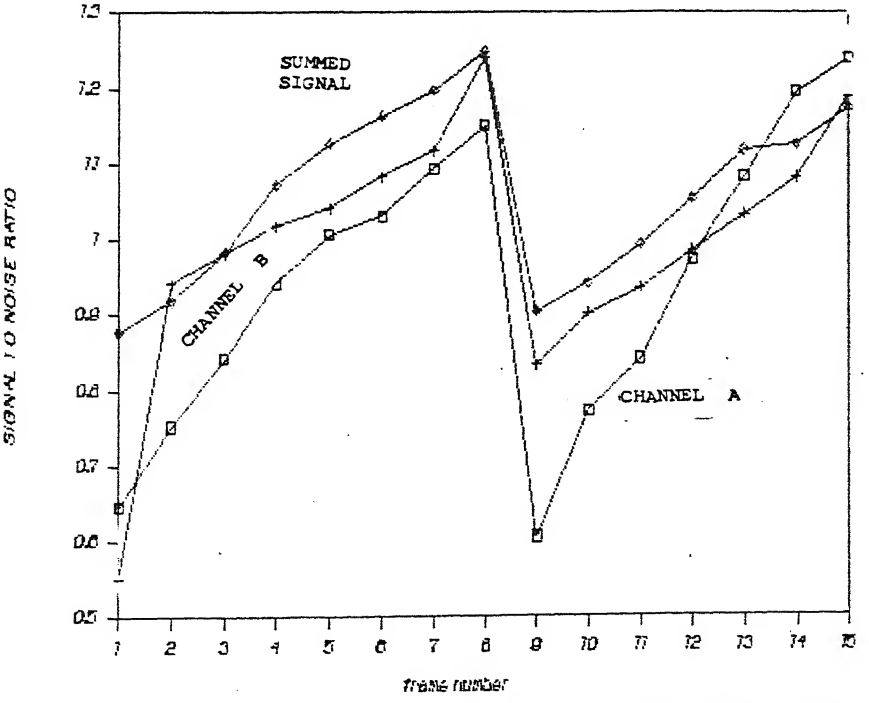

FIG. 3.14 : SIGNAL TO NOISE RATIO OF "EXTENSOR CARPI ULNARIS" FOR CONTRACTION RATE 1 N/sec.

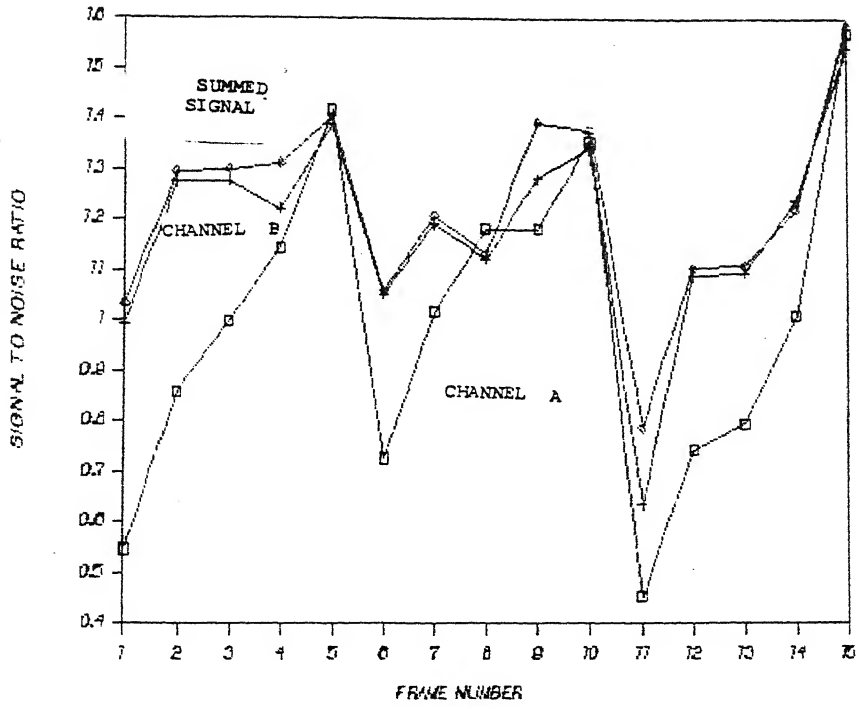

FIG. 3.15 : SIGNAL TO NOISE RATIO OF "EXTENSOR CARPI ULNARIS" FOR CONTRACTION RATE 8 N/sec.

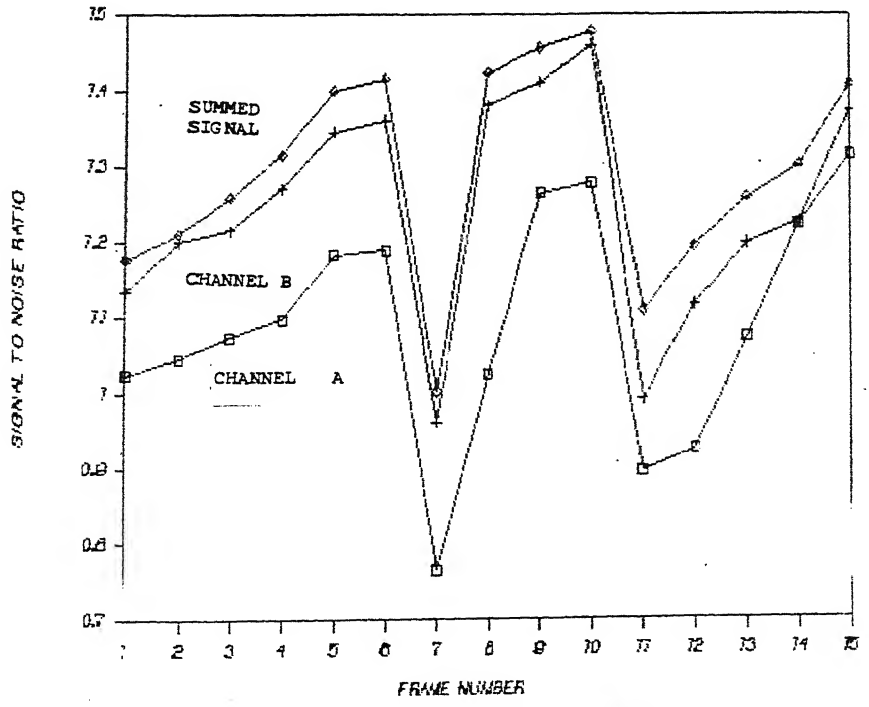

FIG. 3.16 : SIGNAL TO NOISE RATIO OF "EXTENSOR CARPI ULNARIS" FOR CONTRACTION RATE 4 N/sec.

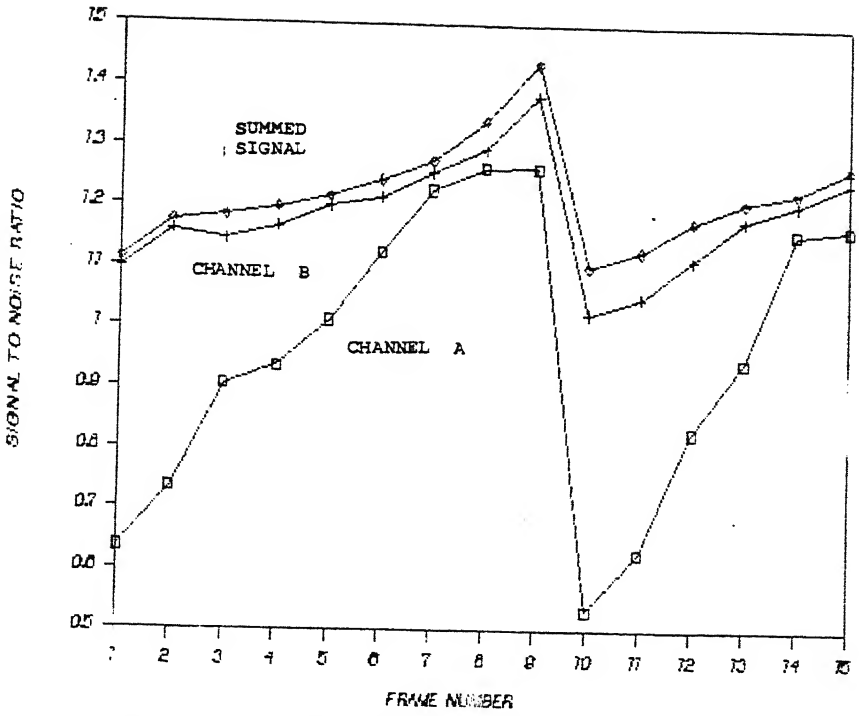

FIG. 3.17 : SIGNAL TO NOISE RATIO OF "EXTENSOR CARPI ULNARIS" FOR CONTRACTION RATE 2 N/sec.

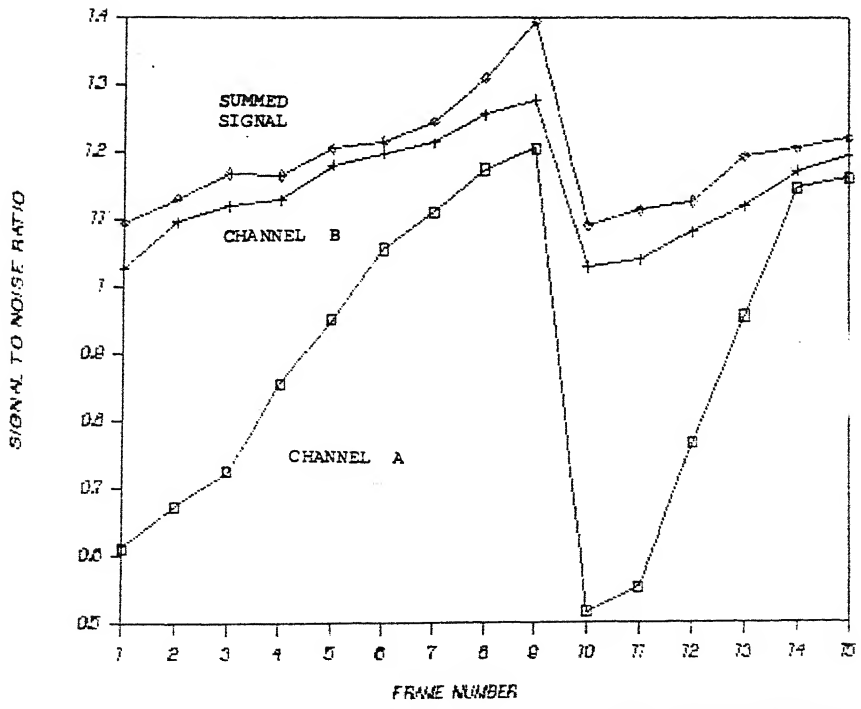

FIG. 3.18 : SIGNAL TO NOISE RATIO OF "EXTENSOR CARPI ULNARIS" FOR CONTRACTION RATE 1 N/sec.

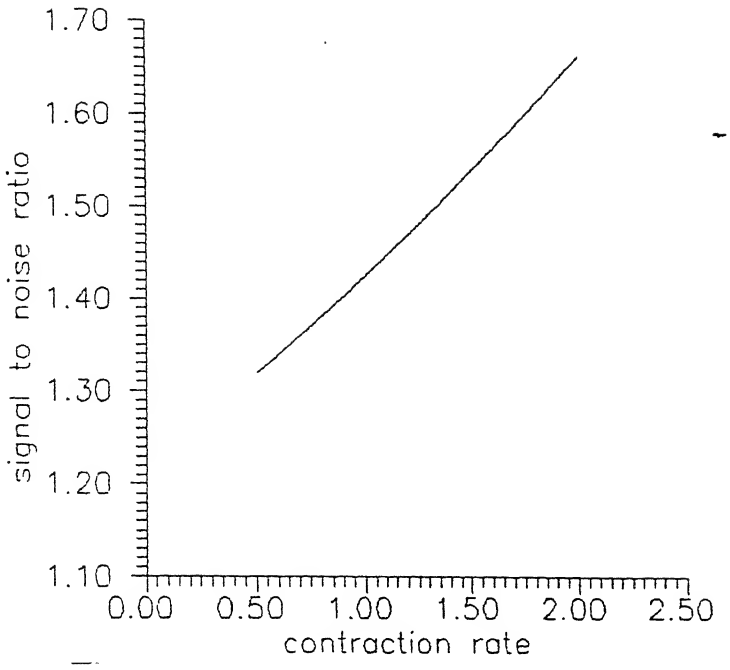

FIG.3.19 : SIGNAL TO NOISE RATIO vs CONTRACTION RATE FOR ABDUCTOR DIGITI MINIMI

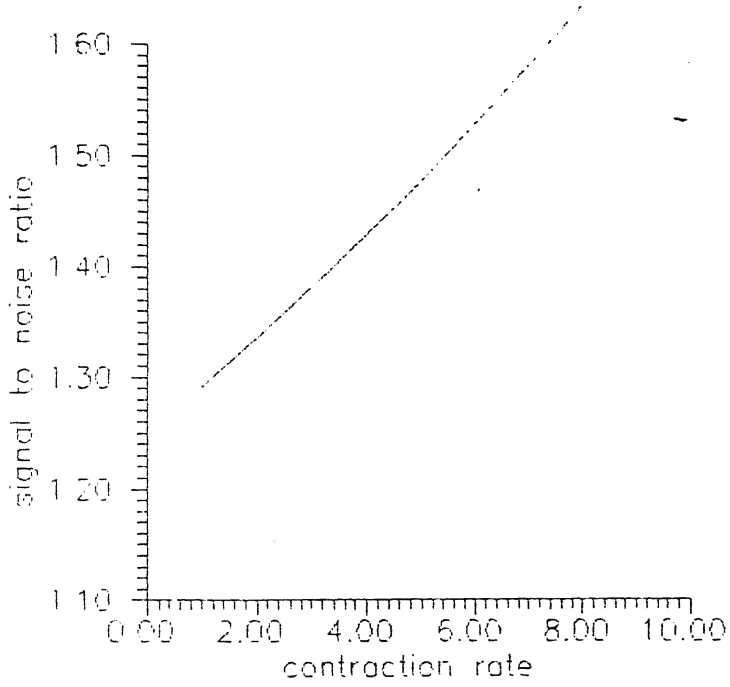

FIG 3.20 : SIGNAL TO NOISE RATIO vs CONTRACTION RATE FOR EXTENSOR CARPI ULNARIS

other pair of electrode. The amount of delay to be given is 10 msec, this is explained as follows. The time period of 50 Hz noise component present in SEMG is 20 msec. When a delay of 10 msec. is given to the SEMG picked up by one electrode pair and is added to SEMG picked up by other electrode pair, the positive peak of noise ofone channel false on negative peak of other channel cancelling the power frequency noise.

3.3.2 The Experiment

The delay was introduced to SEMG pick up of one channel by FFT analyser and both the channel EMGs were stored in memory of FFT analyser. The analysis was carried out on SEMGs picked up at two different contraction rates as shown in Figs. 3.21 to 3.28. The data stored in the memory of FFT analyser were transferred through GPIB interface to IBM.PC.

3.3.3 Resultsand Discussion

The cross correlation coefficient and SNR of the delayed and summed SEMG has been compared with that of without delay and summed SEMG and the results are shown in Tables 3.4 and 3.5.It is evident that there is considerable improvement in the SNR in the case of delayed and summed compared to without delay and summed signal. There is also considerable decrease in cross-correlation coefficient.When the Fourier transform of the delayed and summed signal was

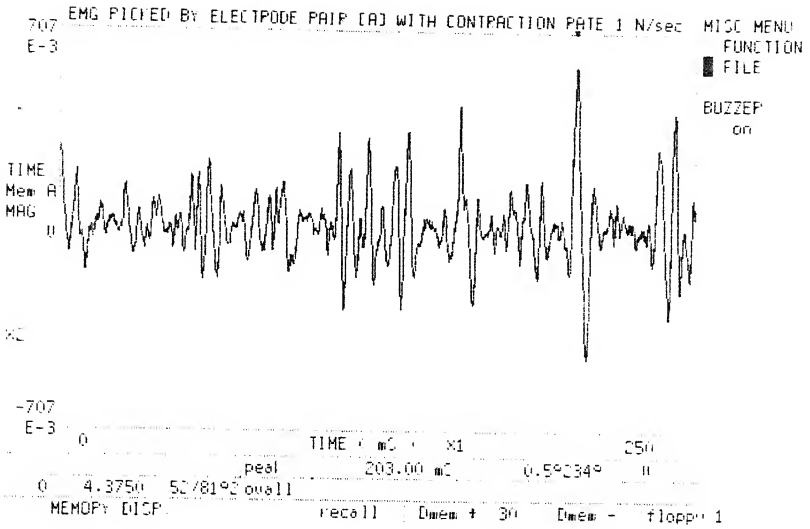

FIG. 3.21 : EMG PICKED UP BY ELECTRODE PAIR A FROM MUSCLE "ABDUCTOR DIGITI MINIMI" FOR CONTRACTION RATE 1 N/sec.

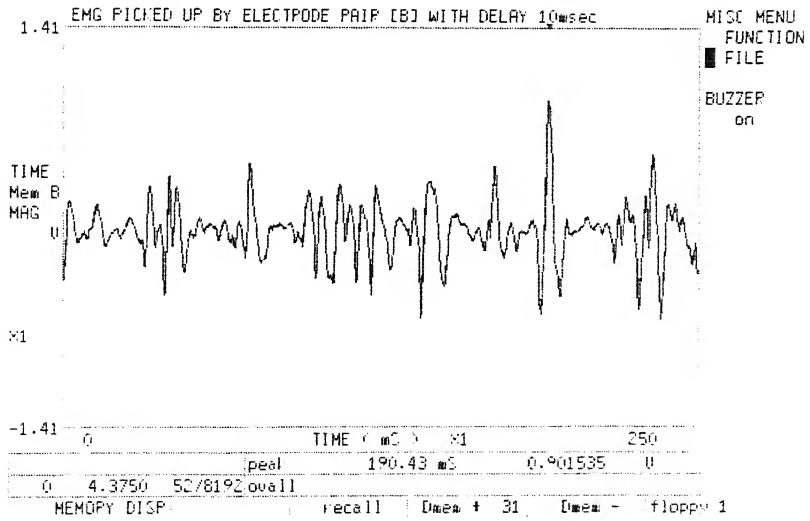

FIG. 3.22 : EMG PICKED UP BY ELECTRODE PAIR B FROM MUSCLE "ABDUCTOR DIGITI MINIMI" FOR CONTRACTION RATE 1 N/sec AND DELAY OF 10 millisec.

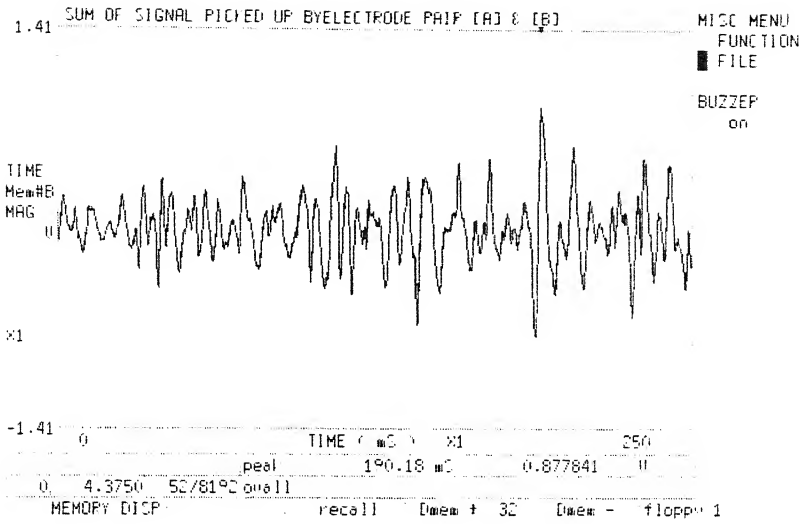

FIG. 3.23 : SUM OF EMG'S PICKED UP BY ELECTRODE PAIRS A AND B WITH CHANNEL B DELAY OF 10 milli-sec.

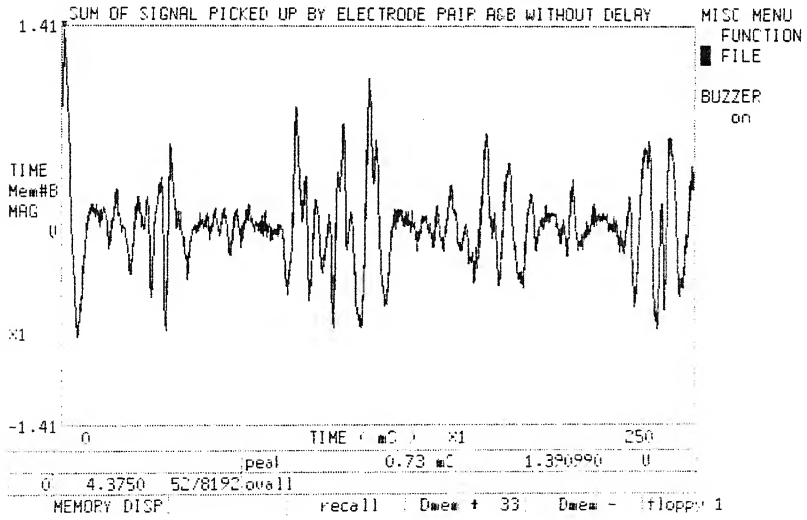

FIG. 3.24 : SUM OF EMG'S PICKED UP BY ELECTRODE PAIRS A AND B WITHOUT DELAY TO CHANNEL B

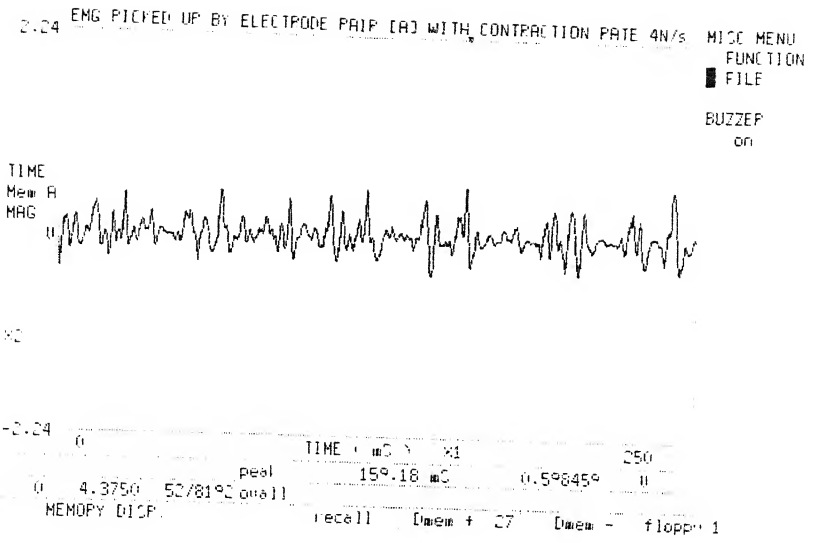

FIG. 3.25 : EMG PICKED UP BY ELECTRODE PAIR A FROM MUSCLE "EXTENSOR CARPI ULNARIS FOR CONTRACTION RATE 4 N/sec.

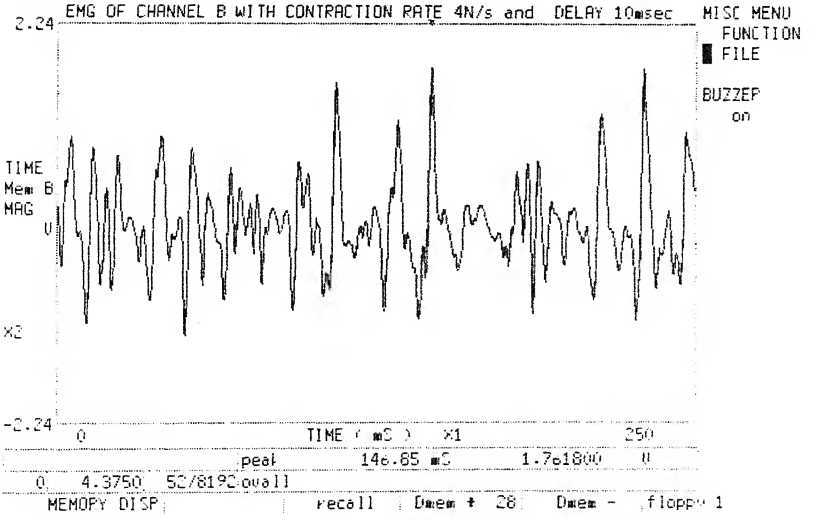

FIG. 3.26 : EMG PICKED UP BY ELECTRODE PAIR B FROM MUSCLE "EXTENSOR CARPI ULNARIS FOR CONTRACTION RATE 4 N/sec AND DELAY OF 10 milli-

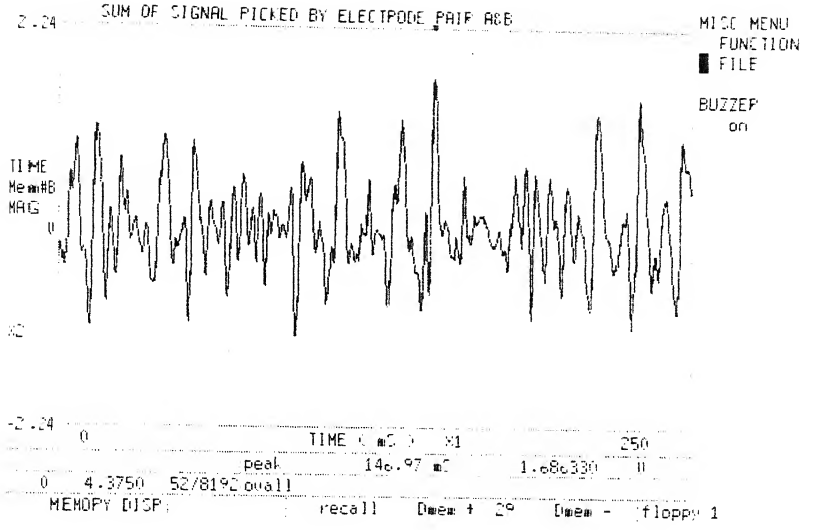

FIG. 3.27 : SUM OF EMG'S PICKED UP BY ELECTRODE PAIRS A AND B WITH CHANNEL B DELAY OF 10 milli-sec.

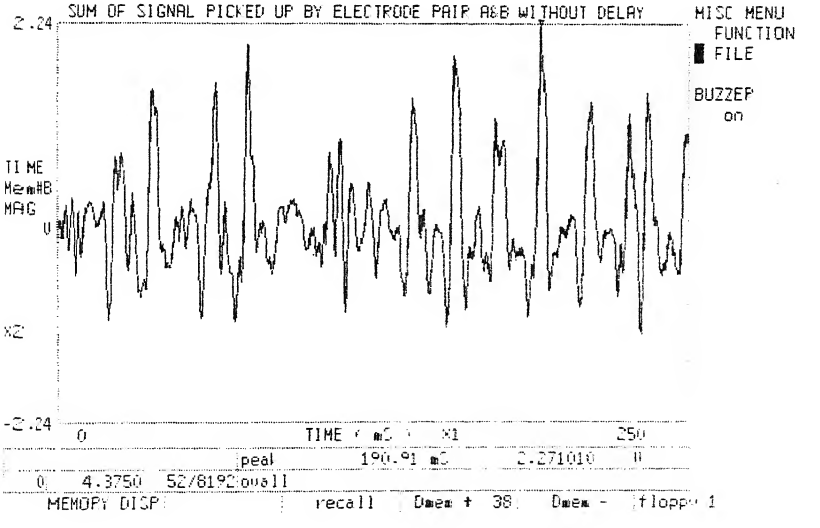

FIG. 3.28 : SUM OF EMG'S PICKED UP BY ELECTRODE PAIRS A AND B WITHOUT DELAY TO CHANNEL B

taken, it was found that the magnitude of 50 Hz frequency component also reduces. The results are shown in Table 3.4 and Table 3.5.

The advantage of this method in SNR improvement is that the SNR which can be obtained using multimyoelectric channel for a given cross correlation coefficient, the same value of SNR can be obtained using two channels and delay circuit. This reduces the difficulty in placing multiple electrode pairs on small muscle and also reduces the circuit complexity.

In the present experiment using two channels and delay of 10 msec. the SNR and cross correlation coefficient were 1.172 and 0.04 respectively for muscle contraction rate of 2 N/sec. For the same value of SNR and using multimyoelectric channel it requires 6 channels (when compared with Fig. 3.29, results obtained by Zhang, Parker, Scott [28] using multimyoelectric channel).

TABLE 3.4 : Signal to Noise Ratio of SEMG Picked-up from "ABDUCTOR DIGITI MINIMI" for Contraction Rate 1N/sec.

	Mean (μ) (V)	Standard deviation (V)	Signal to Noise Ratio	Cross correlation coefficient (ρ)	Magnitude of 50 Hz frequency component in signal
Channel [A]	0.1124	0.1090	1.031	-	0.0167
Channel [B] with delay	0.3692	0.3276	1.126	-	0.0135
Summed signal with delay in channel [B]	0.3741	0.3190	1.172	0.043	0.0099
Channel [A]	0.1124	0.1090	1.031	-	0.021
Channel [B]	0.3832	0.3552	1.078	-	0.0407
Summed signal without delay in channel [B]	0.4493	0.4048	1.109	0.239	0.0585

TABLE 3.5 : Signal to Noise Ratio of SEMG Picked-up from "EXTENSOR CARPI ULNARIS" FOR Contraction Rate 4 N/sec.

	Mean (μ) (A)	Standard deviation (V) ( )	S/N	Cross-correlation coefficient (ρ)	Magnitude of 50 Hz frequency component in signal (V)
Channel [A]	0.1016	0.1192	0.8526	-	0.100
Channel [B] with delay	0.1297	0.1408	0.9231	-	0.113
Summed signal with delay in channel [B]	0.1626	0.1453	1.119	0.081	0.0972
Channel [A]	0.1016	0.1192	0.8526	-	0.023
Channel [B]	0.1728	0.1883	0.9134	-	0.119
Summed signal without delay in channel [B]	0.1986	0.2144	0.9263	0.307	0.138

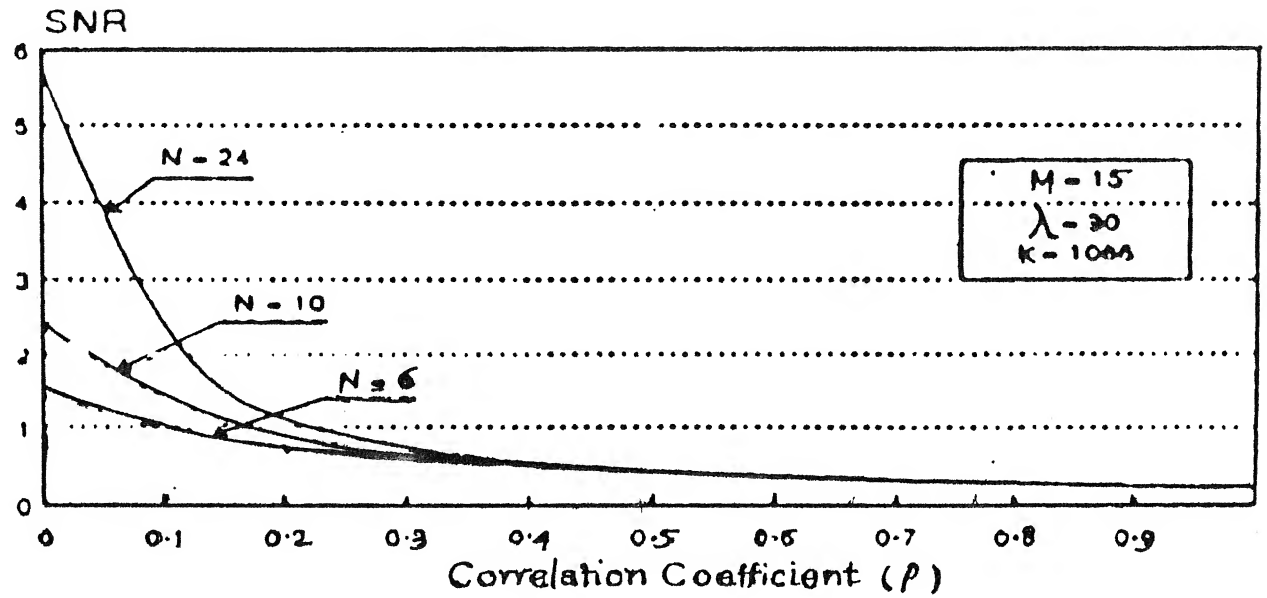

FIG.3.29: Dependence of SNR on the correlation coefficient

CHAPTER - 4

SURFACE EMG AND FORCE CORRELATION FOR NON-ISOMETRIC CONTRACTION

4.1 INTRODUCTION

In prehistoric period cave man used to carry boulders in front (as seen in wall paintings) but present day field workers are seen carrying load on their back also. In order to find out the stress-strain distribution on human skeleton and the most suitable posture of carrying load, a suitable device to measure force during dynamic condition is necessary. Surface emg is one of the easiest way of measuring muscular force during locomotion. The peak to peak amplitude of action potential increases with increasing force. It has been explained in Chapter - 1 that integrated electrical activity is having a near linear relationship with muscular force in case of isometric contraction. Mathematical models explaining this near linear relationship is available owning to its importance in practical application such as proportional control of the gripping force of a prosthetic hand, dentistry etc.

Under dynamic condition the muscle length changes and the contraction is non-isometric. A passive elastic

tension is developed in the muscle which is to be subtracted from the total measured force to obtain the force of contraction developed in the muscle. It is difficult to measure this passive elastic tension developed in the muscle. So, instead of giving a mathematical model showing the effect of firing frequency, recruitment and rate coding (explained in Chapter - 1) on force of voluntary contraction in case of non-isometric contraction, an attempt was made to determine muscular force from directly measuring ISEMG.

For determining force from ISEMG a suitable black box has to be placed between ISEMG as input and force as output. The transfer function of this black box is to be determined. When ISEMG picked up during dynamic condition is passed through this black box, the resulting output gives the measure of muscular force. The block diagram of the model is shown in Fig. 4.1.

The realization of the transfer function can be done using both analog and digital technique.

4.2 THE EXPERIMENT

The experiment was carried on two different muscle, one small "abductor digiti minimi" and other medium sized "extensor carpi ulnaris". The reason for selection of these muscles has been explained in Chapter - 1. The force exerted by muscle and ISEMG were recorded at different muscle contraction rates.

For the realization of transfer function of the black box, the ISEMG and force recorded at different muscular contraction rates of two different muscle were studied. The ISEMG and force exerted by muscle for two different contraction rates are shown in Figs.4.15,4.19,4.23 and 4.24.

The autocorrelation of force and ISEMG are shown in Fig. 4.5 and Fig. 4.6. The cross correlation between ISEMG and force exerted by muscle is shown in Fig. 4.7.

In almost all cases it was found that the ISEMG saturrates for gradually increasing force, Fig. 4.8 and Fig.4.11 (the force is increasing linearly). This has been explained with suitable mathematical model for isometric contraction. The ISEMG is to be linearized so that it approximately represent the muscular force.

4.3 ANALOG CIRCUIT REALIZATION

The plot of force Vs. ISEMG is shown in Fig. 4.2. The mathematical expression which is found to fit the curve is given by

$$F = \exp (3.833 \; E_m) * 0.2226$$

The realization of this force Vs. ISEMG relation was done by antilog amplifier in which ISEMG serves as input and the resulting output which is linear, represents muscular force.

The block diagram of antilog amplifier is shown in Fig. 4.3 and the circuit realization is shown in Fig.4.4.

A_1 and A_2 are operational amplifier with infinite input resistance and zero differential input voltage

$$V_2 = -V_f + V_1$$

$$= - V_T (\ln I_f - \ln I_o) + \frac{R_1}{R_1 + R_2} V_s \qquad (1)$$

V_2 is the negative of the voltage across D_2.

$$V_2 = - V_T (\ln I_2 - \ln I_o) \qquad (2)$$

Combining eq. (1) and eq. (2)

$$V_s \frac{R_1}{R_1 + R_2} = V_T \ln \frac{I_f}{I_2} = V_T \ln \frac{I_f R'}{V_o} \qquad (3)$$

Since $V_o = I_2 R'$

from eqn. (3) it follows that

$$V_o = R' I_f \ln^{-1} - V_s \left(\frac{R_1}{R_1 + R_2} \frac{1}{V_T}\right) \qquad (4)$$

Comparing eqn. (4) with the force-ISEMG relation, values of

I_f = 300 milli-amp, R_1 = 3.3K , R_2 = 5.1K,

R' = 33 Ohm.

Since the input voltage to the antilog amplifier is

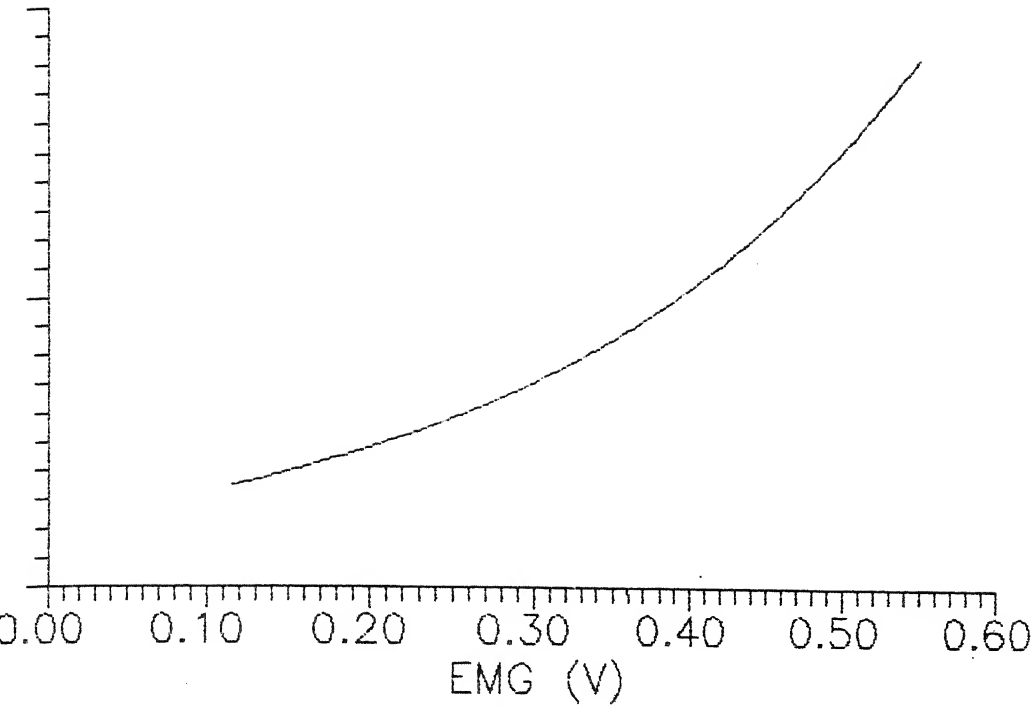

G.4.2: Plot of FORCE vs EMG

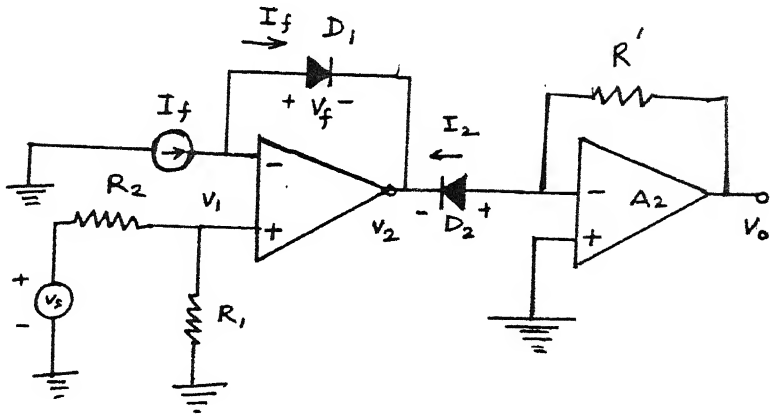

FIG. 4.3

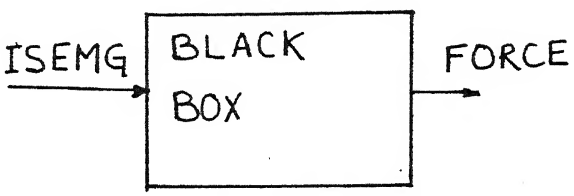

FIG. 4.1

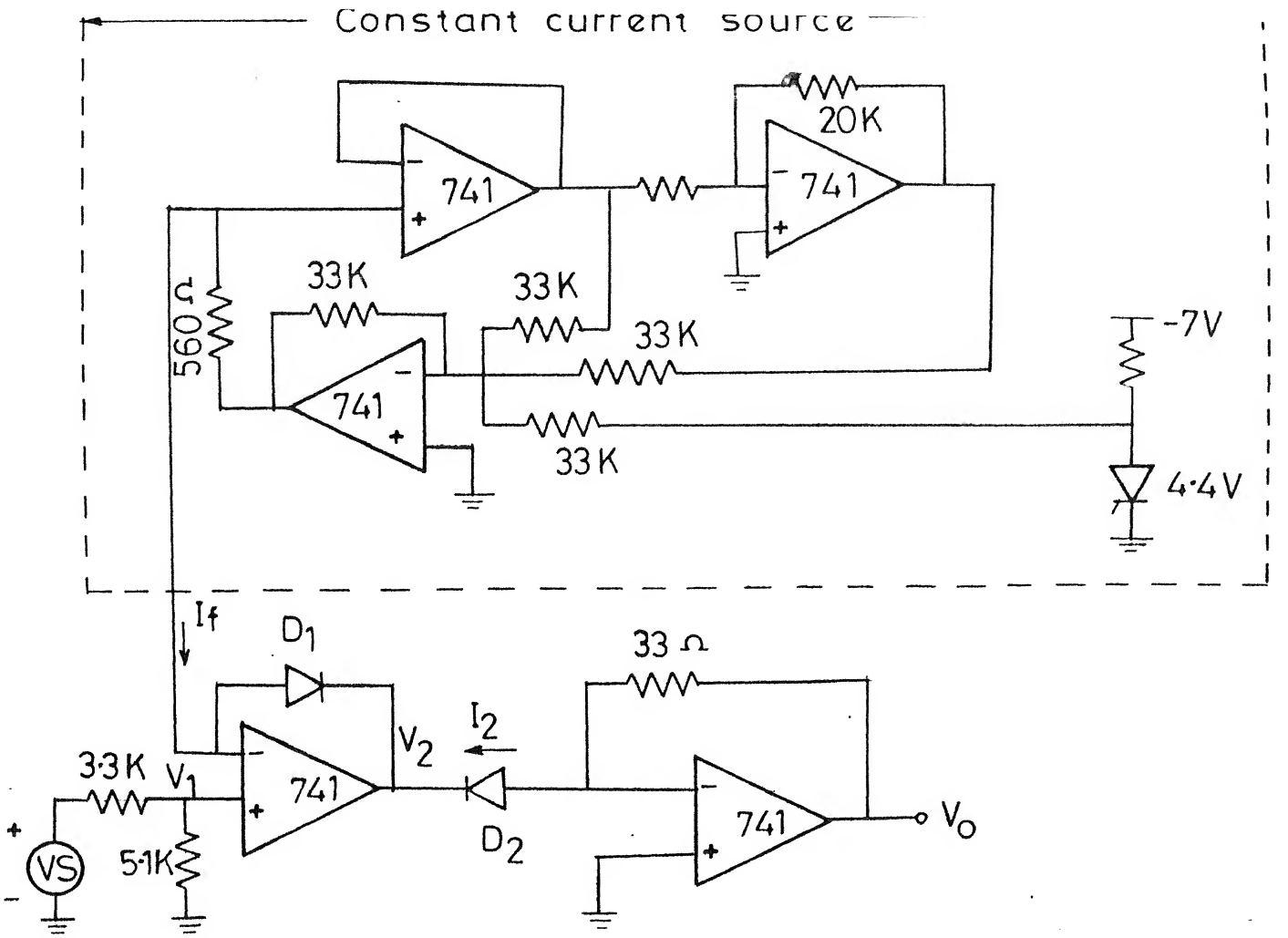

FIG. 4.4 ANTILOG AMPLIFIER

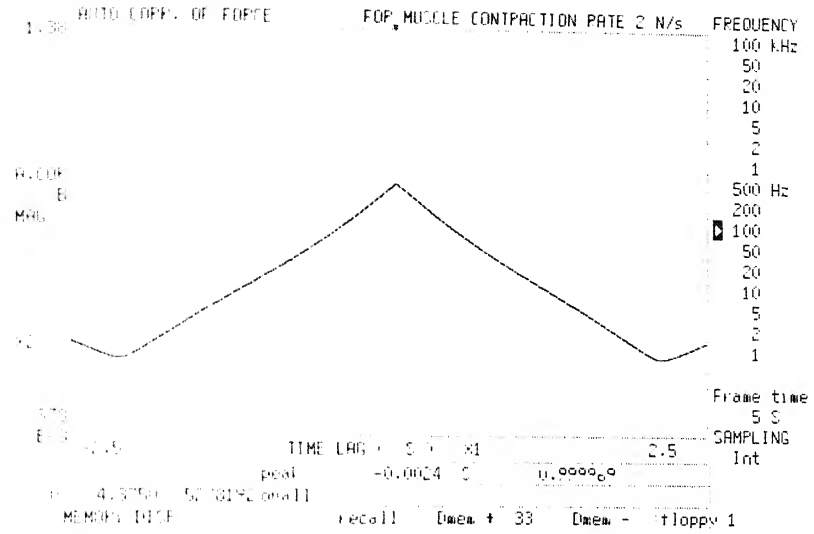

FIG. 4.5 : AUTO CORRELATION OF FORCE

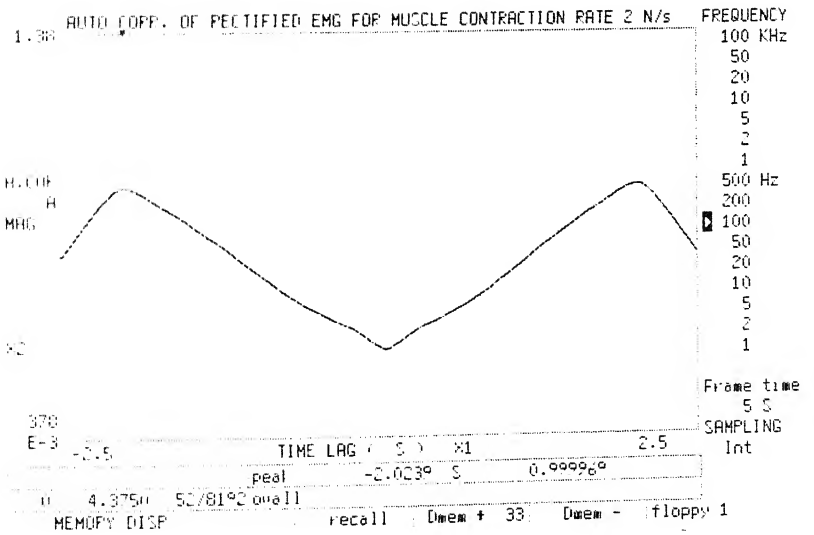

FIG. 4.6 : AUTO CORRELATION OF ISEMG

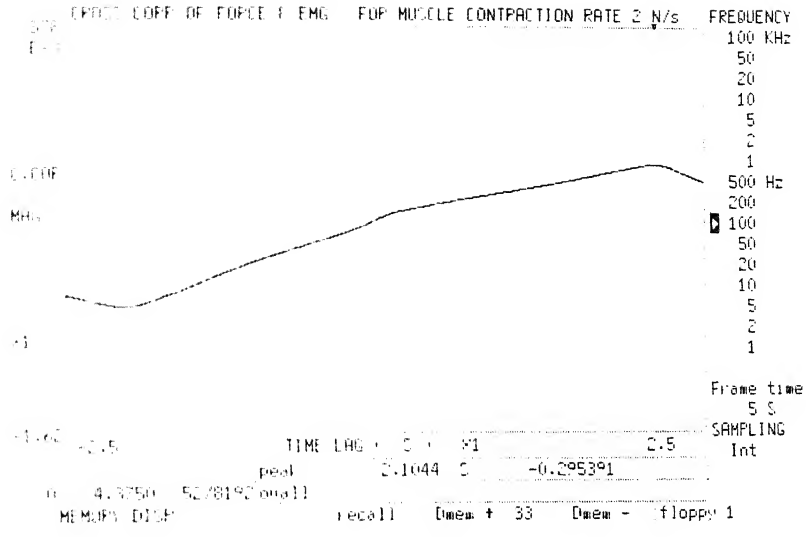

FIG. 4.7 : CROSS CORRELATION BETWEEN FORCE AND EMG FOR MUSCLE CONTRACTION RATE OF 2N/sec.

limited between 0 to 100 mV, the ISEMG was attenuated and given as input. ISEMG recorded at two different muscular contraction rates were given as input to antilog amplifier, Fig. 4.8 and Fig. 4.11 and the resulting outputs are shown in Fig. 4.9 and Fig. 4.12. It is seen that ISEMG gets linearized. When the output of antilog amplifier (Fig.4.9) for a given ISEMG as input (Fig. 4.8) is compared with the force recorded (Fig. 4.10) during experiment using force recorder, it is seen that they are of similar nature.

4.4 DIGITAL TECHNIQUE FOR THE REALIZATION OF TRANSFER FUNCTION

The transfer function of black box in which ISEMG serves as input and force is output is shown in Fig.4.13 for muscle contraction rate of 4 N/sec . The transfer function was found using FFT analyser. The approximate nature of transfer function is shown with dotted line in Fig. 4.13. The general nature of transfer function is shown in Fig. 4.14. This transfer function could be realized using digital filter technique and stored in memory of microcomputer. Taking the Fourier transform of digitized ISEMG and multiplying it with the transfer function, gives the Fourier transform of the force and its inverse Fourier transform gives muscular force. This was done with ISEMG picked up at different muscle contraction rates. ISEMG for muscle contraction rates of 4 N/sec and 2 N/sec. are shown in Fig. 4.15 and Fig. 4.19. The

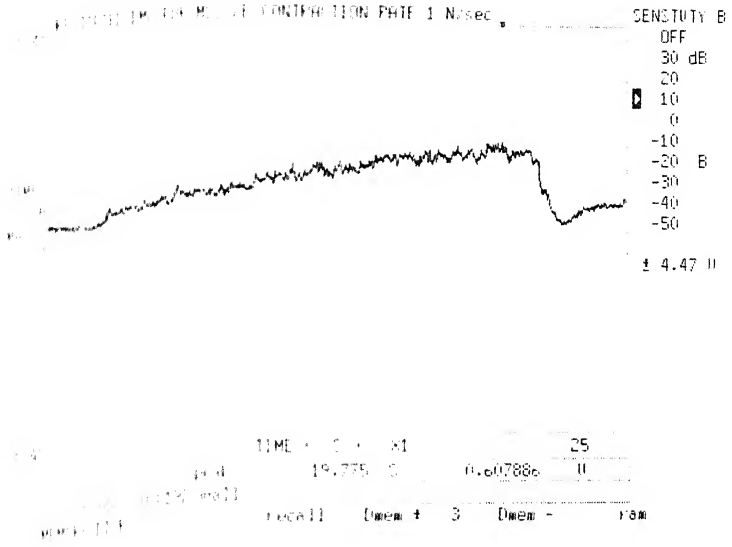

FIG. 4.8 : RECTIFIED AND LOW PASS FILTERED EMG PICKED UP FROM MUSCLE "ABDUCTOR DIGITI MINIMI" FOR MUSCLE CONTRACTION RATE OF 1 N/sec.

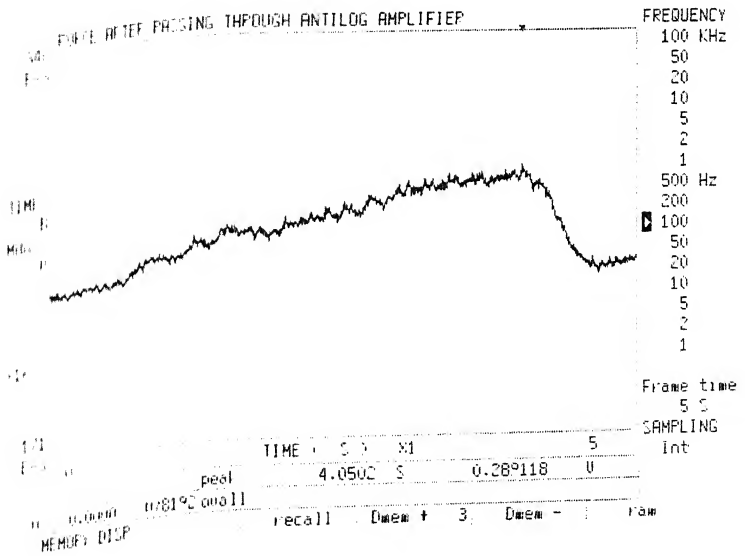

FIG. 4.9 : FORCE AFTER PASSING ISEMG THROUGH ANTILOG AMPLIFIER.

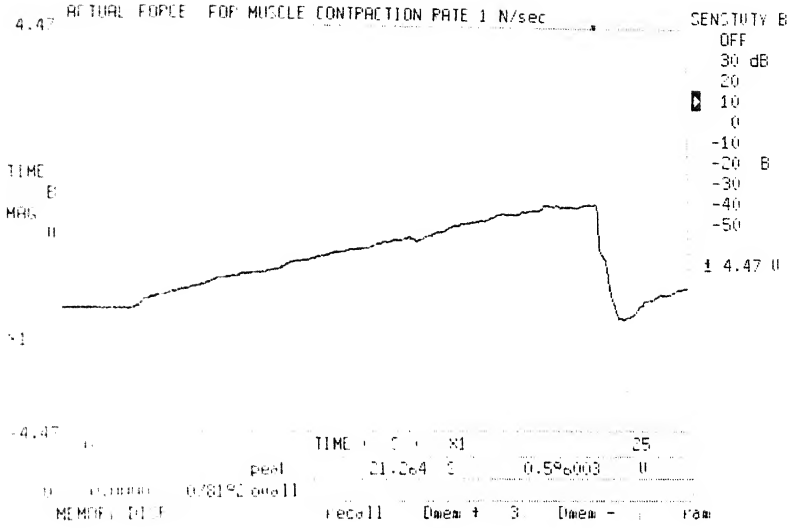

FIG. 4.10 : ACTUAL FORCE RECORDED DURING EXPERIMENT

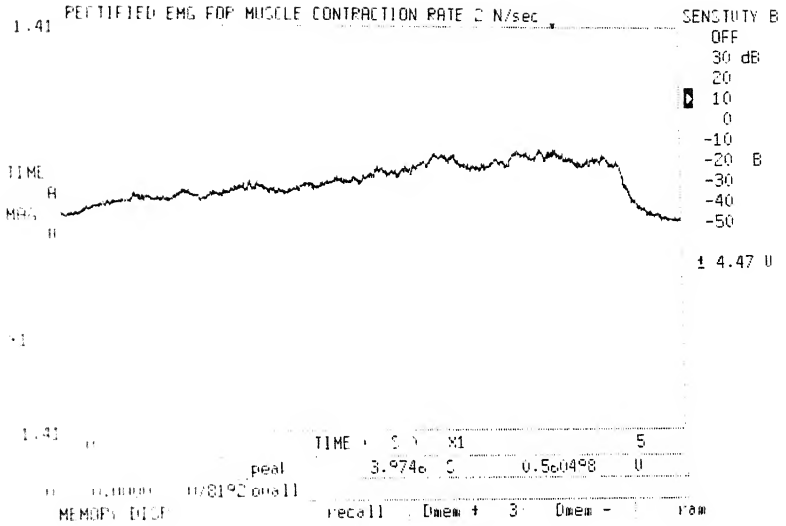

FIG. 4.11 : RECTIFIED AND LOW PASS FILTERED EMG PICKED UP FROM MUSCLE "EXTENSOR CARPI ULNARIS" FOR MUSCLE CONTRACTION RATE OF 2 N/sec.

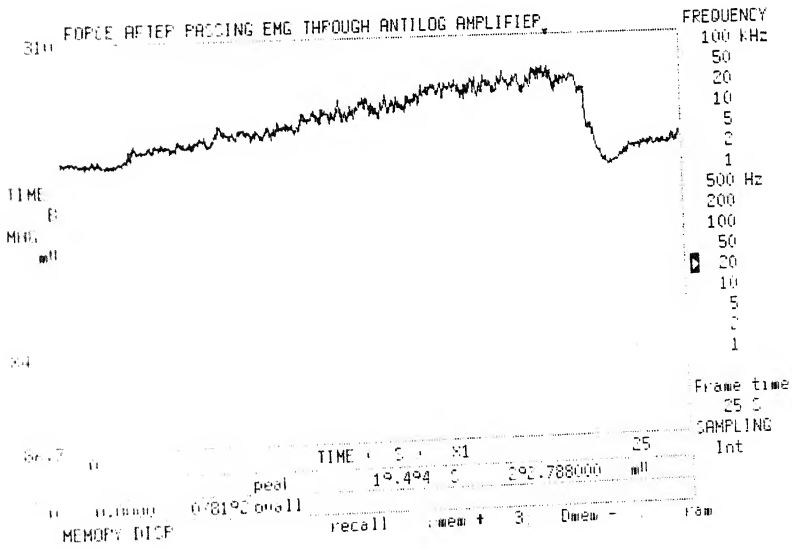

FIG. 4.12 : FORCE -- AFTER PASSING ISEMG THROUGH ANTILOG AMPLIFIER.

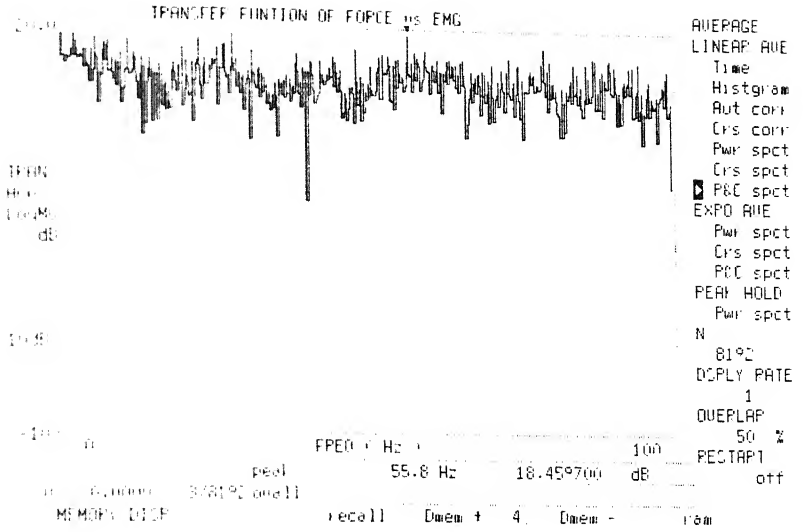

FIG. 4.13 : TRANSFER FUNCTION OF BLACK BOX

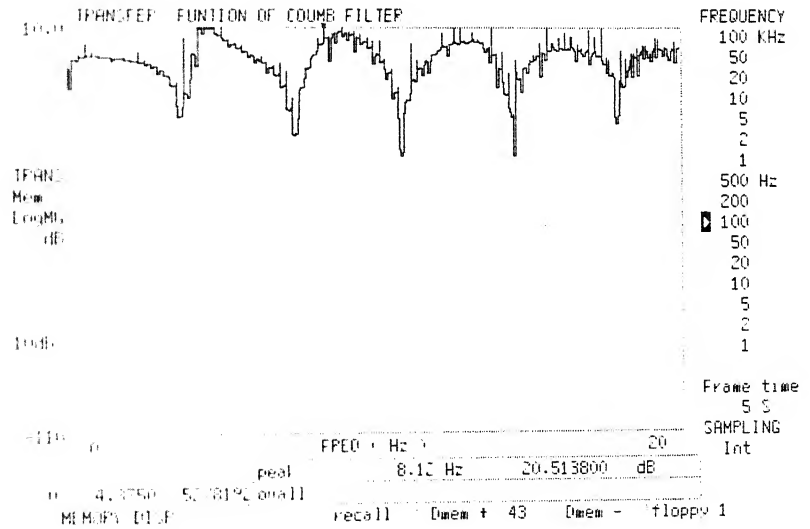

FIG. 4.14 : APPROXIMATE NATURE OF TRANSFER FUNCTION

results of above stated procedure are shown in Fig. 4.15 to Fig. 4.22. It is found that force determined using ISEMG (Fig. 4.18 and Fig. 4.22) is very similar to actual force recorded during experiment (Fig. 4.23 and Fig. 4.24).

4.5 DISCUSSION

The transfer function of the black box found using both analog and digital technique, can serve as a suitable device for measuring muscular force from ISEMG picked up during locomotion.

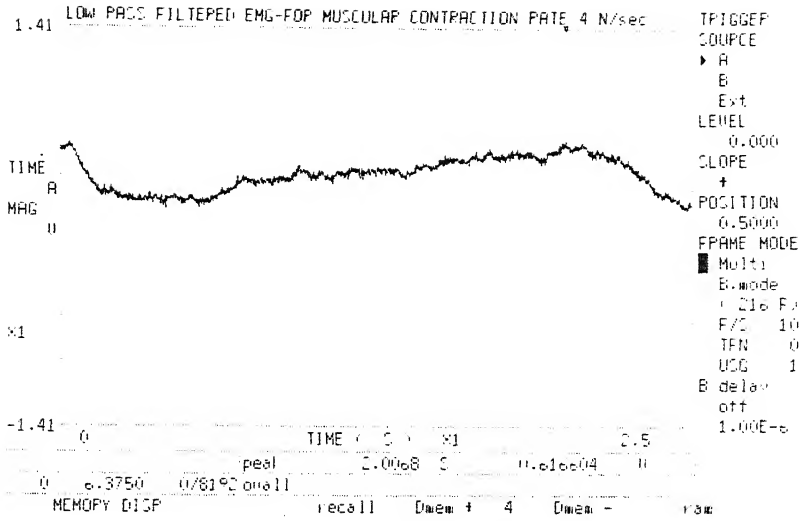

FIG. 4.15 : LOW PASS FILTERED EMG PICKED UP FROM MUSCLE "EXTENSOR CARPI ULNARIS" WITH MUSCLE CONTRACTION RATE 4 N/sec.

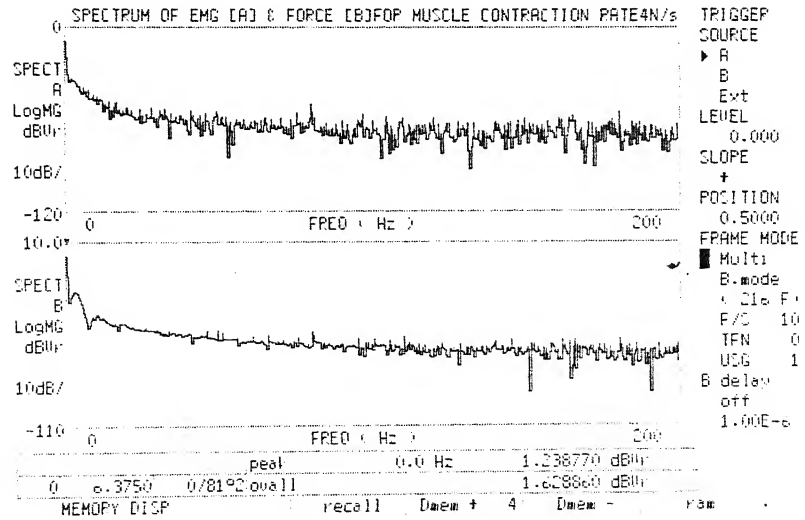

FIG. 4.16 : SPECTRUM OF EMG (TOP) AND FORCE (BOTTOM)

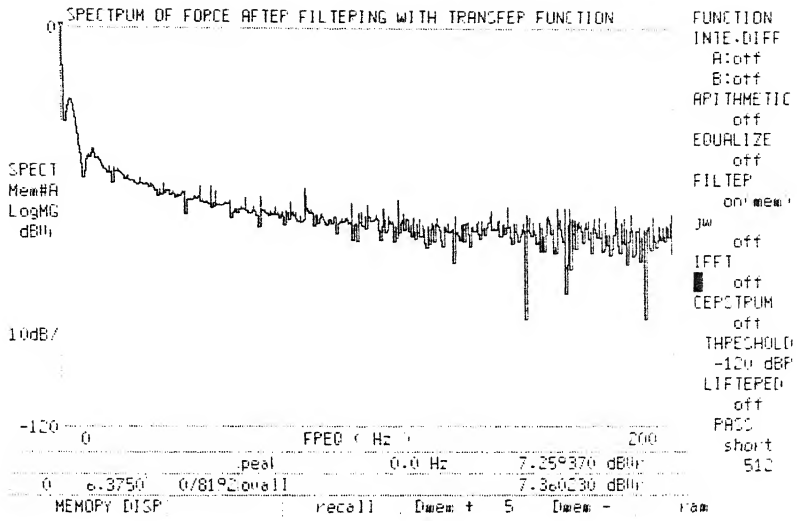

FIG. 4.17 : SPECTRUM OF FORCE AFTER FILTERING THE SPECTRUM OF SEMG

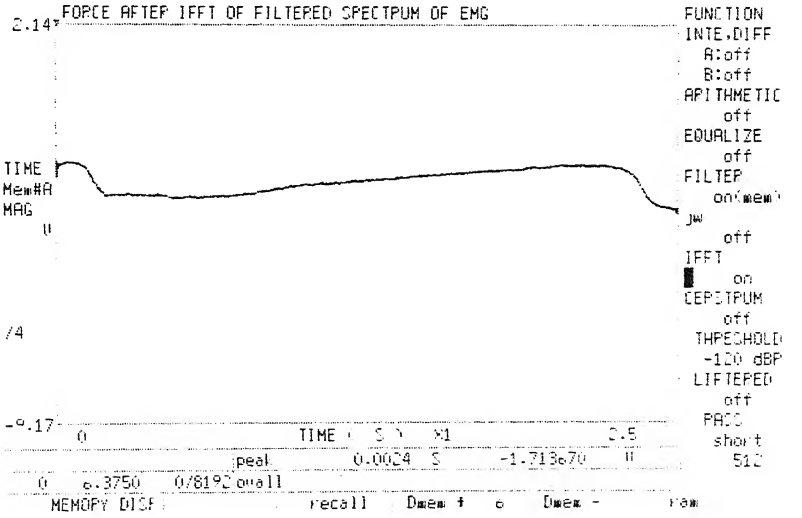

FIG. 4.18 : FORCE AFTER IFFT OF FILTERED SPECTRUM OF EMG

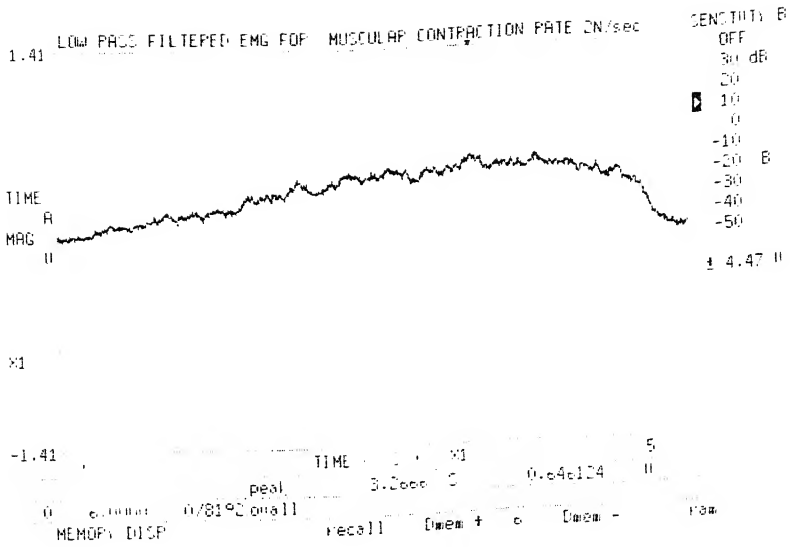

FIG. 4.19 : LOW PASS FILTERED EMG PICKED UP FROM MUSCLE "ABDUCTOR DIGITI MINIMI" WITH MUSCLE CONTRACTION RATE 4 N/sec.

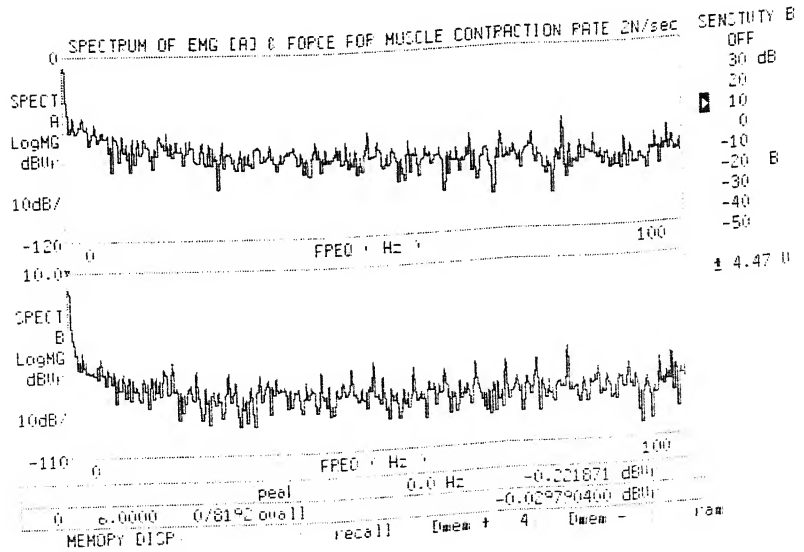

FIG. 4.20 : SPECTRUM OF EMG (TOP) AND FORCE (BOTTOM)

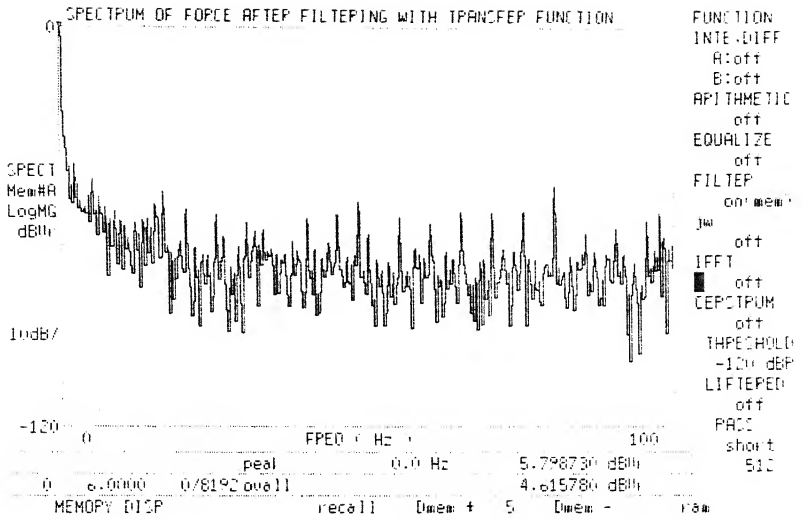

FIG. 4.21 : SPECTRUM OF FORCE AFTER FILTERING THE SPECTRUM OF SEMG

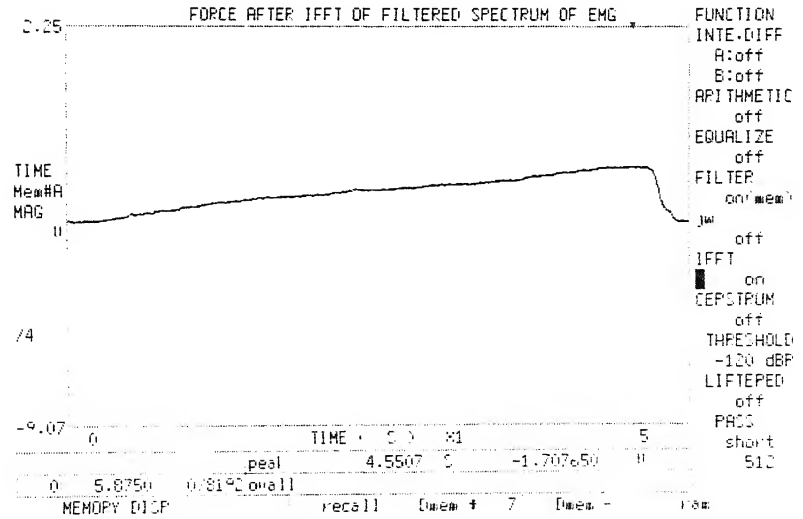

FIG. 4.22 : FORCE AFTER IFFT OF FILTERED SPECTRUM OF EMG

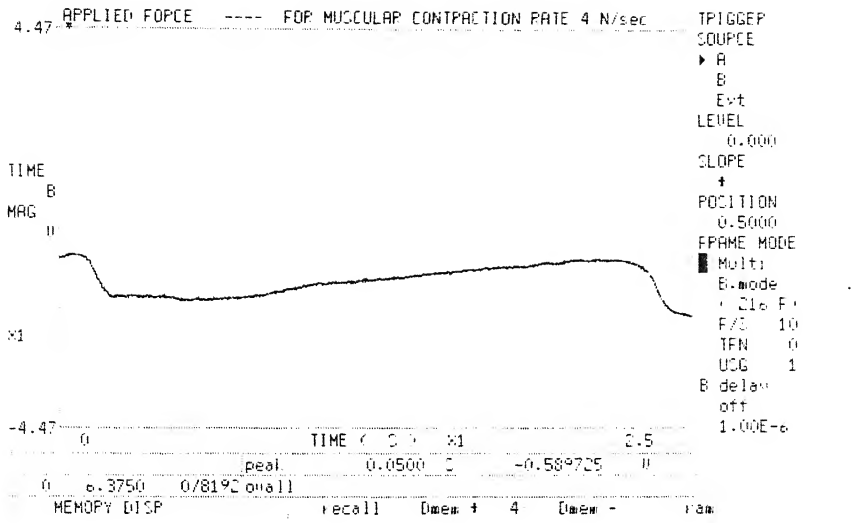

FIG. 4.23 : APPLIED FORCE-RECORDED DURING EXPERIMENT FOR RATE 4 N/sec.

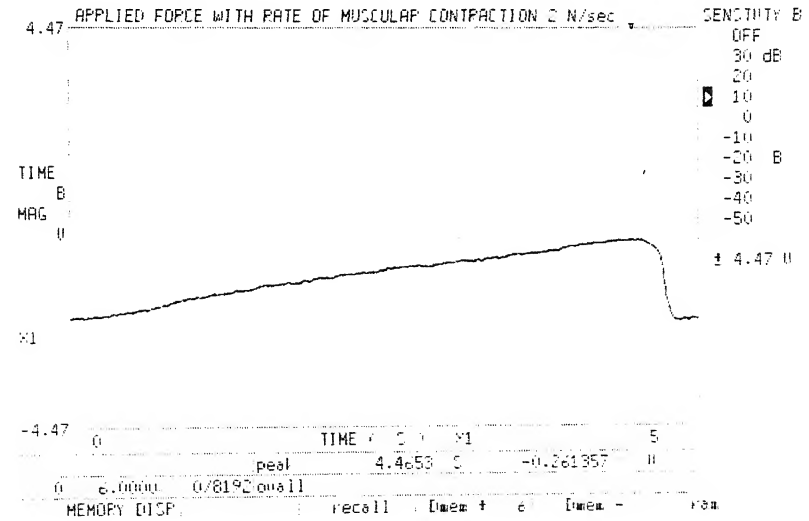

FIG. 4.24 : APPLIED FORCE-RECORDED DURING EXPERIMENT FOR RATE 2 N/sec.

CHAPTER - 5

SCOPE OF FURTHER WORK

The basic objective of finding muscular force and ISEMG correlation under non-isometric contraction of muscle is to determine muscular force by measuring SEMG. It has been explained earlier that during locomotion almost all muscle contractions are non-isometric. So, the transfer function model provided in the present work can serve as a suitable device for measuring force.

Along with lifting and pushing and pulling, load carrying is a very common manual materials handling task. The metabolic energy requirements for different methods of load carrying have been studied under a variety of conditions. The general principle that has evolved from these studies is that in order to minimize energy expenditure the load should be located as closely as possible to the centre of mass of the subject. The total metabolic energy expenditure measurements provide no indication of local loading of particular muscles such as the muscles of the lower back. It is possible that a particular activity may require only a moderate increase in total metabolic energy but cause fatigue in a local muscle group that has to produce high contractile level as part of accomplishing that activity. The amount of EMG output can be used as a measure of the relative tension in the muscle and from this, assessment could be made how different load

and position affect myogenic spinal joint compression and muscular fatigue.

For the avoidance of low back problems investigations can be done regarding proper lifting technique, body posture and maximum acceptable load of lifting. One of the possible contributing factors to injury is the effect of neuromuscular interaction in situations in which the individual has no knowledge of load magnitude prior to the actual lift attempt. Investigations can be done to determine the relationships among variables typically associated with lifting in order to minimize individual muscle forces and joint stresses. Studies can also be done to see whether past experience on specific task alters the muscular coordination and enhances overall movement skill by changing muscle action in a given situation.

REFERENCES

1. SHWEDYK, E., BALASUBRAMANIAN, R., SCOTT, R.N., (1977), A non-stationary model for the electromyogram, IEEE Trans. on Bio-Medical Engg.; Vol. BME-24, No. 5, Sept.

2. CLAMMAN, H.P. (1967), A quantitative analysis of firing pattern of single motor units of skeletal muscle of man and their utilization on isometric contraction, Ph.D. Thesis, John Hopkin's University, Baltimore, Md.

3. BASMAJIN, J.V. (1962), Introduction in: Muscles alive, Willium and Wilkins, Baltimore, pp. 16-40.

4. MILNER-BROWN, H.S., STEIN, R.B., YEMM, R. (1973), Changes in firing rate of human motor units during linearly changing voluntary contraction, J. Physiology, Vol. 230, pp. 371-390.

5. SUCKLING, E.E. (1962), Skeletal muscles in bio-electricity, 160-179, McGraw Hill.

6. MILNER-BROWN, H.S., STEIN, R.B. (1975), The relation between the surface electromyogram and muscular force, J. Physiology, Vol. 246, pp. 549-569.

7. MILNER-BROWN, H.S., STEIN, R.B., YEMM, R. (1973), The orderly recruitment of human motor units during voluntary isometric contraction, J. Physiology, Vol. 230, pp. 359-370.

8. ELDRED, E. (1960), 'Posture and Locomotion', in Handbook of Physiology, Section-1, Neurophysiology, Vol. 11, Editor-in-chief J. Field, American Physiological Society, Washington, D.C., pp. 1072-74.

9. VREDENBREGT, J., KOSTER, W.G. (1966), Some aspects of muscle mechanism in vivo, I.P.O. report, Institute for perception research, Eindhoven, Holland.

10. ZUNIGER, E.N., SIMMONS, D.G. (1969), Non-linear relationship between averaged electromyogram potential and muscle tension in normal subjects, Archives of physiological medicine and rehabilitation, Vol. 50, pp. 613-620, Nov.

11. SHWEDYK, E. (1974), Estimation of a muscle's force from its myoelectrical signal during non-isometric contraction Ph.D. Thesis, Univ. of New Brunswick, Fredericton, N.B.

12. BROBECK, J.R. (1973), Excitation and Contraction of muscles, Best and Taylor's Physiological Basis of Medical Practice, 9th Ed., Willium and Wilkins Co. Baltimore, pp. 1-104, 1-106.

13. OLSON, C.B., CARPENTER, D.O., HENNEMAN, E. (1968), Orderly recruitment of muscle action potentials, Arcns. Neurol. Psychit. London, 19, pp. 591-597.

14. YEMM, R. (1977), The orderly recruitment of motor units of the masseter and temporal muscles during voluntary isometric contraction in man, J. Physiol. 265, pp. 163-174.

15. DESMEDT, J.E., GODAUS, E. (1977), Ballistic contractions in man: Characteristic recruitment pattern of single motor units of the Tibialis Anterior Muscle, J. Physiol. 264, pp. 673-693.

16. RAY, G.C., GUHA, S.K. (1983), Relationship between the surface e.m.g. and muscular force, Medical and Biological Engineering & Computing, pp. 579-585, September.

17. PERSON, R.S., MISHIN, L.N. (1964), Auto and Cross-correlation analysis of the electrical activity of muscles, Med. & Biol. Engg., 2, 155-159.

18. O'DONNEL, R.D., RAPP, J. BERKHOUT, J., ADEY, W.R. (1973), Autospectral and coherence patterns from two locations in the contracting biceps, Electromyography clin. Meurophysiol. 13, 259-269.

19. RUCH, T.C., FUTTON, J.F. (1960), Medical physiology and biophysics, 18th edition, W.B., Saunders Company.

20. BIGLAND, B., LIPPOLD, O.C.J. (1954), The relation between force, velocity and integrated electrical activity in human muscles, J. Physiology, 123, pp. 214-224.

21. BERNSHTEIN, V.M. (1967), Statistical parameters of the electrical signal of a muscle model, Biophysics, 12, 801-13.

22. LIBKIND, M.S. (1968), Modelling of interference bio-electrical activity-II, Biophysics, 13, pp. 811-821.

23. PERSON, R.S., LIBKIND, M.S. (1969), Simulation of electromyograms showing interference patterns, Electro-encephalography and clin. Neurophysiology, 28, pp. 625-636.

24. KREIFELDT, J.G. (1969), An analysis of surface-detected EMG as amplitude modulated noise and logarithmic dete-ction, Proc. of the 8th Inter. Conf. on Med. & Biol. Rngg., Chicago-III, Session 7-6.

25. ZHANG, Y.T., PARKER, P.A. AND SCOTT, R.N., 1989, A correlated multi-myoelectric channel model and its SNR characteristics, IEEE Eng. in Med. & Bio., 11th Annual Int. Con.

26. SATJARTHIP THUSNEYAPAN, GEORGE I. ZAHALAK, 1989, A practical electrode-array myoprocessor for surface electromyography, IEEE Trans. on Bio. Engg., Vol. 36, No. 2, February.

27. JOHN G. KREIFELDT AND SUMNER YAO, 1974, A signal-to-noise investigation of nonlinear electromyographic processors, IEEE Trans. on Bio. Engg., Vol. BME-21, No. 4, July.